THE EFFECT OF COPPER ON THE MICROSTRUCTURE AND AGING CHARACTERISTICS OF AN 0.8%C BAINITIC STEEL

A THESIS SUBMITTED TO
THE GRADUATE SCHOOL OF NATURAL AND APPLIED SCIENCES
OF
MIDDLE EAST TECHNICAL UNIVERSITY

BY

ÇAĞATAY YILDIRIM

IN PARTIAL FULFILLMENT OF THE REQUIREMENTS
FOR
THE DEGREE OF MASTER OF SCIENCE
IN
METALLURGICAL AND MATERIALS ENGINEERING

DECEMBER 2022

Approval of the thesis:

THE EFFECT OF COPPER ON THE MICROSTRUCTURE AND AGEING CHARACTERISTICS OF AN 0.8%C BAINITIC STEEL

submitted by **ÇAĞATAY YILDIRIM** in partial fulfillment of the requirements for the degree of **Master of Science in Metallurgical and Materials Engineering Department, Middle East Technical University** by,

Prof. Dr. Halil Kalıpçılar
Dean, Graduate School of **Natural and Applied Sciences** _____

Prof. Dr. Ali Kalkanlı
Head of the Department, **Metallurgical and Materials Eng** _____

Prof. Dr. Bilgehan Ögel
Supervisor, **Metallurgical and Materials Eng**, METU _____

Examining Committee Members:

Prof. Dr. Rıza Gürbüz
Metallurgical and Materials Eng, METU _____

Prof. Dr. Bilgehan Ögel
Metallurgical and Materials Eng, METU _____

Prof. Dr. Arcan F. Dericioğlu
Metallurgical and Materials Eng, METU _____

Prof. Dr. Ender Keskinkılıç
Metallurgical and Materials Eng., Atılım University _____

Assist. Prof. Dr. Eda Aydoğan Güngör
Metallurgical and Materials Eng, METU _____

Date: 02.12.2022

I hereby declare that all information in this document has been obtained and presented in accordance with academic rules and ethical conduct. I also declare that, as required by these rules and conduct, I have fully cited and referenced all material and results that are not original to this work.

Name Last name: Çağatay Yıldırım

Signature:

ABSTRACT

THE EFFECT OF COPPER ON THE MICROSTRUCTURE AND AGING CHARACTERISTICS OF AN 0.8%C BAINITIC STEEL

Yıldırım, Çağatay
Master of Science, Metallurgical and Materials Engineering
Supervisor: Prof. Dr. Bilgehan Ögel

December 2022, 64 pages

Copper causes hot shortness in steel. However, the 1:2 nickel-to-copper ratio avoids hot shortness phenomena. Also, it is known that an aging treatment applied to ferritic steels causes age hardening via the precipitation of Cu in the form of BCC copper-rich clusters. The latter phenomenon was studied extensively in low and medium-carbon steels. In this study, the copper precipitation in bainitic high-carbon steel and its effect on microstructure and properties are investigated. To achieve this, 0.8% C steel having 2% copper and 1% nickel was cast and isothermally heat treated at various temperatures to obtain bainite. Then the bainitic steels were aged at various temperatures and times. Copper could not suppress carbide precipitation and as a result, retained austenite phase could not be detected in bainitic structures. However, aging retards further softening of the bainite structure in comparison to martensitic specimens.

Keywords: Isothermal Heat Treatment, Bainite, Copper, Aging

ÖZ

BAKIRIN %0.8C BEYNİTİK ÇELİĞİN İÇYAPISI VE YAŞLANDIRMA ÖZELLİKLERİNE ETKİSİ

Yıldırım, Çağatay
Yüksek Lisans, Metalurji ve Malzeme Mühendisliği
Tez Danışmanı: Prof. Dr. Bilgehan Ögel

Aralık 2022, 64 sayfa

Bakır, çelikte sıcak gevrekliğe neden olur. Bununla birlikte, 1:2 nikel-bakır oranı sıcak gevreklik fenomenini önler. Ayrıca, ferritik çeliklere uygulanan yaşlandırma işleminin, bakırın, gövde merkezli kübik yapıda bakırca zengin kümeler halinde çökelmesi yoluyla yaşlandırma sertleşmesine neden olduğu bilinmektedir. İkinci fenomen, düşük ve orta karbonlu çeliklerde kapsamlı bir şekilde incelenmiştir. Bu tez çalışmasında, mukavemet-süneklik dengesini kaybetmeden mukavemette daha fazla artışı araştırmak için beynitik yüksek karbonlu çelikte bu fenomen incelenmiştir. Bunun için, %2 bakır ve %1 nikel içeren %0,8 C çelik döküldü ve beynit elde etmek için çeşitli sıcaklıklarda izotermik ısıl işleme tabi tutuldu. Daha sonra beynitik çelikler çeşitli sıcaklık ve sürelerde yaşlandırılmıştır. Bu çalışma sonucunda bakır, karbür çökelmesini bastıramadı ve sonuç olarak beynitik yapılarda bulunan östenit fazı tespit edilemedi. Ancak yaşlandırmanın martensitik numunelere kıyasla beynitik yapının daha fazla yumuşamasını geciktirdiği görülmüştür.

Anahtar Kelimeler: İzotermal Isıl İşlem, Beynit, Bakır, Yaşlandırma

To my beloved family

ACKNOWLEDGMENTS

I wish to express my deepest gratitude to my supervisor Prof. Dr. Bilgehan Ögel, for his guidance, patience, criticism, encouragement, and insight throughout the research.

Special thanks to Prof. Dr. Ali Kalkanlı for the casting of the steel used in this study.

I would also like to thank Zafer Yıldırım for his suggestions, comments, and valuable friendship.

In this acknowledgment inscription, it is not possible to ignore Emin Taylan. SEM images would not have been appropriately obtained without his guidance.

Additionally, I would like to thank research assistant Mustafa Balcılar for his support and helpful criticisms.

Finally, I would like to express my greatest thank to my parents, brother, sister-in-law, and my little niece for their love and moral support.

TABLE OF CONTENTS

LIST OF TABLES

TABLES

LIST OF FIGURES

FIGURES

LIST OF ABBREVIATIONS

ABBREVIATIONS

CCT: Continuous Cooling Transformation

TTT: Time Temperature Transformation

M: Martensite

B: Bainite

Mf: Martensite Finish Temperature

Ms: Martensite Start Temperature

Bs: Bainite Start Temperature

RA: Retained Austenite

M/A: Martensite/Austenite

HV30: Vickers Hardness Scale with 30 kg Application

CHAPTER 1

INTRODUCTION

Steel is accepted as one of the basis for today's civilization. Its easy recyclability, availability, and moderately good mechanical properties make it indispensable among other metals. Even though, in the last few decades, nonferrous alloys and composite materials have gained a large place in the industry, energy efficiency and environmental issues brought to mind the question of whether steel will regain its former importance. Moreover, in recent years, the strength-ductility balance has become an essential parameter in industry, and iron alloys are moderately good in this parameter [1].

In steels and other metals, as strength increases, toughness decreases by considering most of the strengthening mechanisms [2]. Only grain refinement can enhance strength and toughness together [3]. Moreover, brittle phases like carbides should be suppressed to preserve strength-toughness balance [3,4]. Therefore, if high-strength material with high toughness is desired, the material must have a fine-grained and carbide-free microstructure which requires energy-consuming complex heat treatment procedures and expensive additives as in maraging steels [5]. However, previous studies about the bainitic steels requiring less complicated heat treatment procedures and cheaper additives show the strength-toughness level of carbide-free bainite with the thin film of retained austenite among bainitic ferrites starts to catch that of maraging steels [4,6].

As known, a certain amount of copper in steel causes ductility and hot-forming problems [7]. The amount of copper in steel is expected to increase and exceed tolerable limits due to recycling problems brought about by the fact that copper is less oxidizable than steel [8]. Despite this bad trend and negative aspects of copper,

there are positive findings too. These are: 1:2 nickel-to-copper ratio in steel prevents hot shortness phenomena [9], and copper precipitation within ferrite grain strengthens the material without decreasing toughness[10].

Copper precipitation characteristics, its effects on bainite transformation, and mechanical properties were studied by various researchers for low and medium-carbon steels, but these topics were not studied well in high-carbon steels.

In this thesis study, high carbon steel specimens containing a reasonable amount of copper and nickel were heat treated to investigate further increasing in strength without losing strength-ductility balance in bainitic steels.

CHAPTER 2

LITERATURE REVIEW

2.1 Martensite

The martensite is the hardest phase in steels which is produced by rapid quenching just after austenitization. Due to the high cooling rate where diffusion of atoms is not allowed, chemical compositions of parent and product phases remain almost the same. Likewise, the parent phase transforms to the product phase with the cooperative movement of atoms which is called military transformation, unlike civilian transformations that require disordered motion of atoms, i.e., transformations with diffusion. Hence martensitic transformations are accepted as diffusionless. As its transformation is diffusionless at a specified temperature, the maximum amount that can be obtained is independent of the time elapsed at that temperature [11]. Moreover, diffusionless transformation restraints the movement of Carbon atoms, and thus it leads to the formation of a BCT lattice structure instead of BCC. Moreover, the axial ratio (c/a) of the BCT lattice is sensitive to the amount of Carbon because of the lattice distortion created by octahedral interstitial sites occupied with Carbon atoms [20]. Therefore, the strength of martensite is much more dependent on the amount of Carbon than other micro constituents [21].

Crystallographic techniques and high-temperature optical microscope experiments have shown that transformation takes place by deformation of the parent austenite phase, as shown in Figure 2.1. This deformation is governed by a large thermodynamic driving force and causes the invariant plane strain consisting of shear and dilatational strain with an undistorted and unrotated interface called the invariant plane [12].

a) 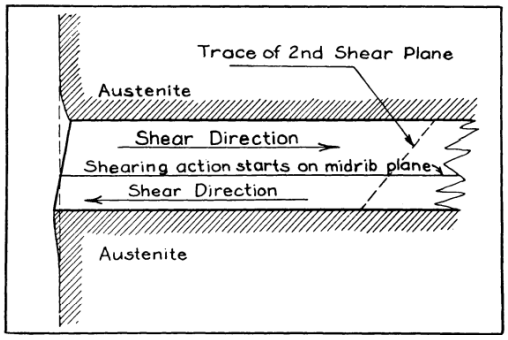

b) 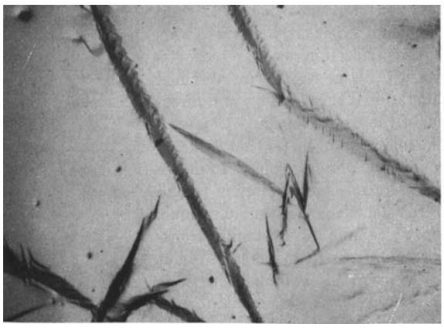

Figure 2.1.a) Schematic formation mechanism of martensite and b) surface tilting on as-polished specimen because of the martensite formation [13]

Martensite can be observed as two major morphologies depending on the chemical composition of the alloy and transformation temperature. Although there are different terms in the literature, these morphologies can be described as lath and plate martensite.

The lath martensite consists of the parallel neighbor laths that form packets as seen in Figure 2.2.a. There may be several packets in prior austenite grains, and these packets may possess different orientations with adjacent packets.

Considering plate martensite, shear resistance should be higher to obtain this morphology. This means alloying elements such as carbon and lower transformation temperature are required to observe plate martensite. Plate martensite does not consist of parallel units, unlike lath martensite, as in Figure 2.2.b. Another feature that distinguishes plate martensite from lath martensite is the twins inside the plate martensite.

In both morphologies, there is high dislocation density, distorted lattice, fine grain, and supersaturated solid solution condition compared with other microstructures that steel may have [22,23].

Although the parameters are not well characterized, these differences are accepted as the reason of high strength and brittleness of martensite [23].

a) 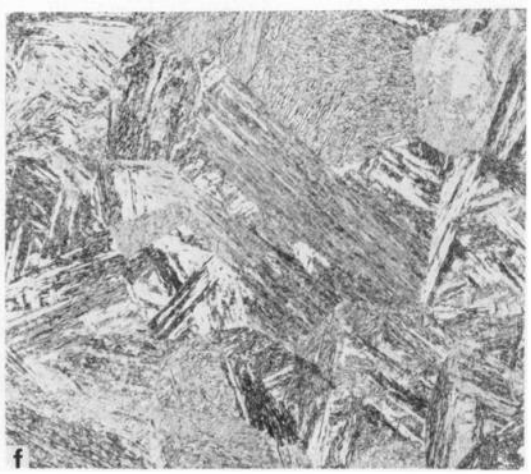 b) 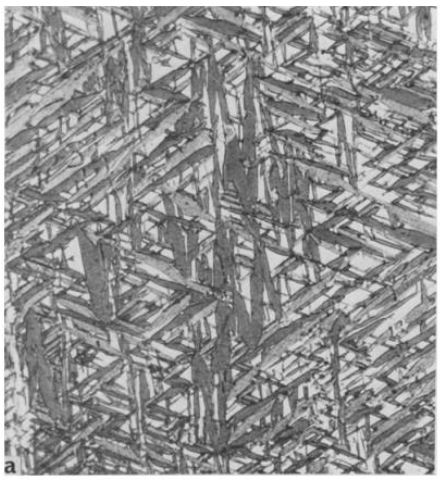

Figure 2.2. a) Lath martensite in Fe-0.2 C (magnified 205 times) b) Plate martensite in Fe-13.9 Mn alloy (magnified 1000 times) [23]

Because of its brittleness, martensitic steels are often tempered to gain toughness in response to decrease in strength. In industry, wide range of strength to toughness ratio can be obtained by changing tempering parameters in martensitic steels [12].

2.2 Bainite

In iron alloys, both toughness and strength can be optimized by increasing the amount of the bainite phase. In bainitic steels, with the help of alloying elements and heat treatments, ultimate tensile strength in the range of 2.0 GPa and toughness of as high as 30 MPa.$m^{1/2}$ can be obtained [14].

Their formation mechanism and microstructure must be examined to understand their balanced strength and toughness. Currently, there are two controversial schools about the bainite formation mechanism. These are displacive and reconstructive transformations. In recent studies, new bainitic steels with outstanding properties were discovered by using displacive theory [28]. In this thesis study, the displacive theory was used to design alloy composition and heat treatment route.

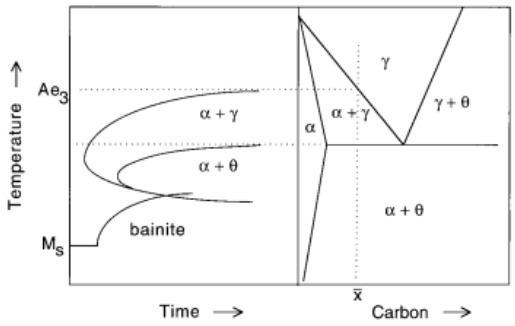

Figure 2.3. The relationship between a TTT and corresponding Fe-C phase diagram [3]

TTT diagrams essentially consist of two C curves, as indicated in Figure 2.3. The upper C curve represents the time required to initiate reconstructive transformations such as ferrite and pearlite, whereas the lower C curve represents displacive transformations such as bainite. [3].

As in martensite transformation, bainite forms by shear deformation of the austenite phase with invariant plane strain; however, unlike martensite, carbon diffuses to the adjacent austenite phase, and carbides can form in bainite subunits or between them because of the higher transformation temperature [6,25].

As can be seen in Figure 2.4, bainite is a nonlamellar aggregate of carbides and plate-shaped ferrite. The ferrite plates are about 10 μm long and about 0.2 μm thick making the individual plates invisible under the optical microscope. Depending on the transformation temperature two kinds of bainite may form. These are upper and lower bainite. During transformation, these micro-constituents form bigger micro-constituents called sheaves. This structure was illustrated in Figure 2.4 [3].

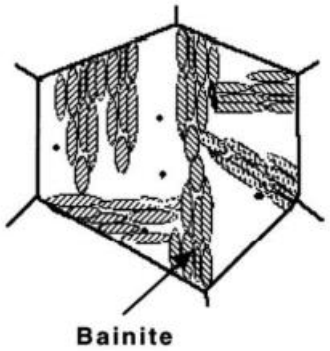

Figure 2.4. Illustration of bainite sheaves and retained austenite [3]

Upper bainite consists of clusters of platelets of ferrite adjacent to each other and cementite particles between them but in lower bainite, cementite particles can be observed within ferrite matrix [11]. The difference between their morphologies can be seen in Figure 2.5. The temperature boundary between upper and lower bainite in isothermal heat treatments was given in Figure 2.6.

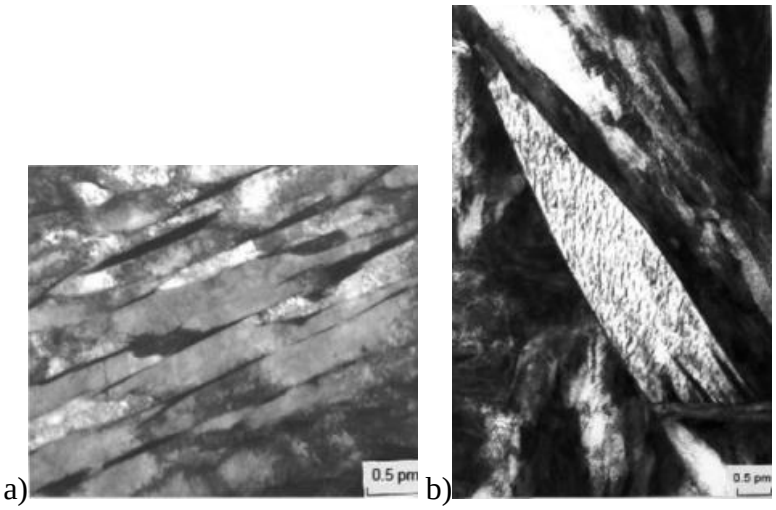

Figure 2.5. Transmission Electron micrographs of a) Upper and b) Lower Bainite [15]

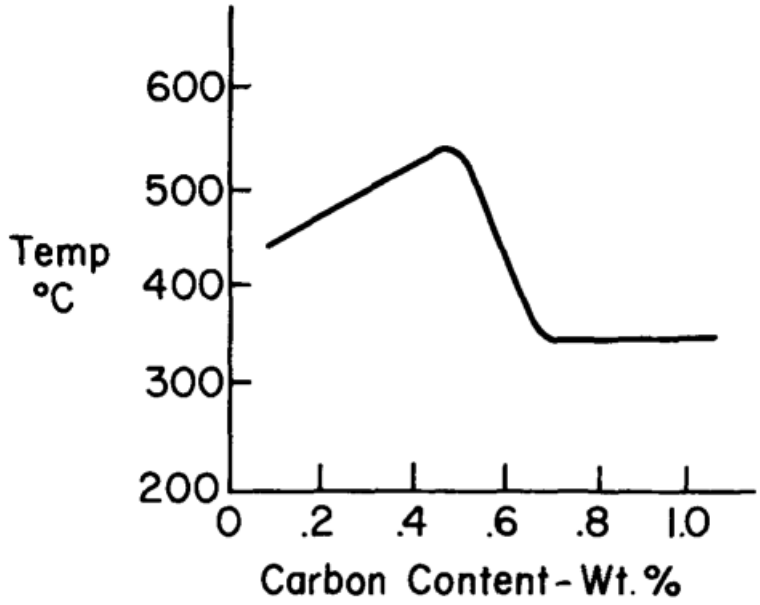

Figure 2.6. The temperature boundary between upper and lower bainite depending on amount of carbon [26]

2.2.1 Design Concept for New Bainitic Steels

In recent years, increasing the toughness and strength of materials simultaneously became important because of the pressure created by the concerns about energy consumption, the automotive and defense industries. As known, strength and toughness are mutually exclusive material properties if most of the strengthening mechanisms are considered [2]. Therefore, a more complex alloy and heat treatment design may be required to increase both properties as indicated in Figure 2.7.

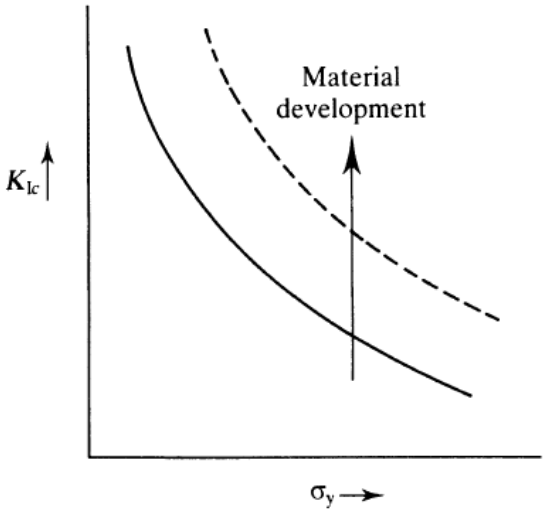

Figure 2.7. Philosophy employed to develop high fracture-toughness & high strength materials [2]

In terms of strength-toughness balance TRIP and Maraging steels occupy top positions [27]. Nevertheless, new bainitic steels designed by using displacive theory seem to catch that level. In these steels, T_0' is shifted to higher carbon levels to prevent blocky retained austenite and carbide precipitation is suppressed by careful alloying and heat treatment design. As a result, in terms of strength-toughness, top ranked alloys can be caught with relatively new design concept in bainitic steels [28]. The place of new bainitic steels was illustrated in Figure 2.8.

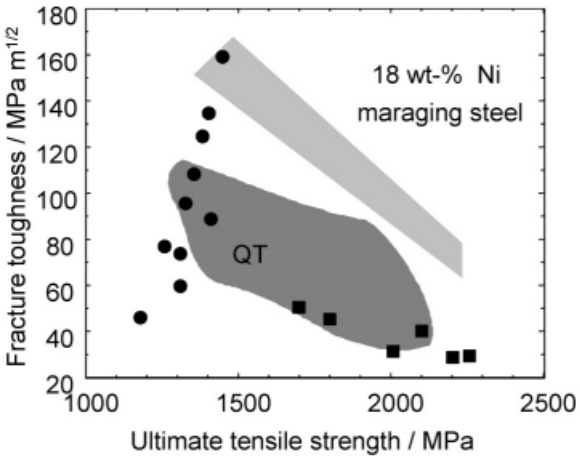

Figure 2.8. Comparison of ultimate strength versus fracture toughness of various steels and bainitic steels (square and circle dots) [29]

2.2.1.1 Thermodynamic Criteria for Bainite Transformation

In transformation, diffusionless growth takes place and austenite carbon concentration at transformation temperature must be lower than T_0 line to obtain bainite microstructure. T_0 line is the boundary where austenite and ferrite Gibbs free energies become equal but as bainitic transformation is displacive ferrites stored energy must be added and therefore T_0 should be modified to T_0'. If T_0' is not considered, instead of bainite, strength reducer blocky retained austenite or Martensite/Austenite regions (M/A) may form [3].

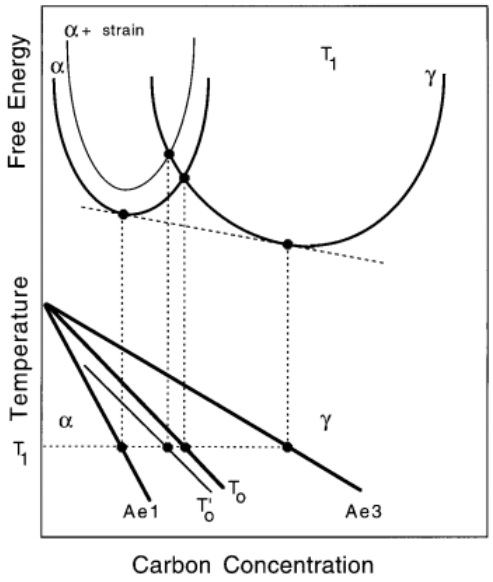

Figure 2.9. T_0 and T_0' curves and their origin [3]

2.2.1.2 Criteria for Carbide Free Bainite

After formation of bainite, cementite between ferrite platelets form. This cementite is responsible for initiating fracture in high strength steels and its absence is expected to increase both toughness and strength [4].

To obtain carbide-free bainite, austenite carbon concentration at transformation temperature must be lower than the para-equilibrium line [33].

The carbide formation can be suppressed by various elements. Well-known, studied by various researchers, and proven experimentally example of these elements is Si. The solubility of Si in cementite is very low therefore it suppresses cementite precipitation as indicated in Figure 2.10 [16].

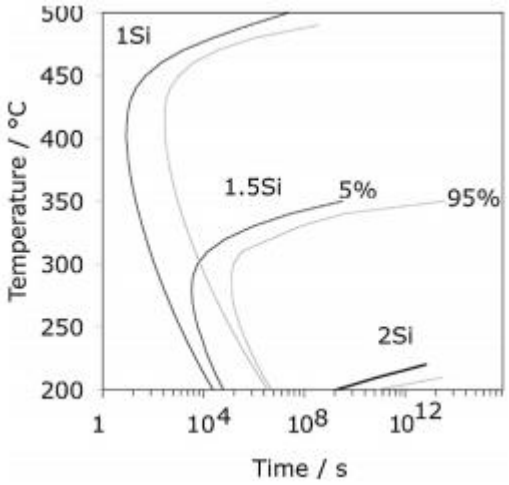

Figure 2.10. Predicted time–temperature–precipitation diagram for para-equilibrium cementite in system Fe–Si–Mn–C with base composition Fe–1.2C–1.5Mn–1.5Si [16]

In addition, effects of carbide free microstructure on mechanical properties can be directly seen. Up to 2 GPa ultimate tensile strength and approximately 6 Joule impact toughness can be obtained by adding Si [17].

2.2.1.3 Superposition of All Criteria for Carbide Free Bainite

To summarize, temperature should be below T_0' curve, to suppress carbide formation carbon concentration should be below para-equilibrium curve and temperature should be above Martensite-start temperature curve to avoid martensite formation. In short, shaded area in Figure 2.11 represents range of parameters for carbide free bainite [33].

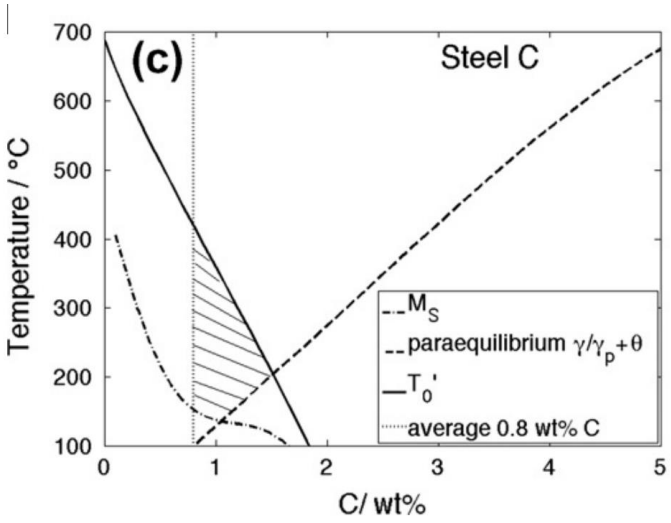

Figure 2.11. T-C diagram [33]

By changing composition of alloying elements, this area can be made bigger. For example,

1. By adding Al, carbide formation can be suppressed and T_0' curve can be shifted to higher carbon concentration values at lower temperatures.
2. By decreasing Mn T_0' curve can be shifted to higher carbon concentration values.
3. By adding Co T_0' curve can be shifted to higher carbon concentration values [33].
4. By adding Si, para-equilibrium curve can be shifted to higher carbon concentration values [16].
5. As C increases, M_s decreases [12].

2.2.2 Copper in Steels

The recycling of scrap metals via Electric Arc Furnace is one of the routes of steel making. Although it is used widely, tramp elements such as copper restricts this production route. If adequate Ni alloying is not provided, Cu may cause hot shortness during hot working [9]. Due to selective oxidation of iron on the surface, Cu enriched phase forms between scale and iron as indicated in Figure 2.12. Moreover, this Cu rich phase has lower melting point than iron. This phase melt during hot working

and weakens grain boundaries. Therefore, it may cause surface cracks during hot working [18]. Furthermore, amount of copper in the steel that produced with EAF is expected to increase with time and exceed tolerable limits due to recycling problems brought about by the fact that copper is less oxidizable than steel [8].

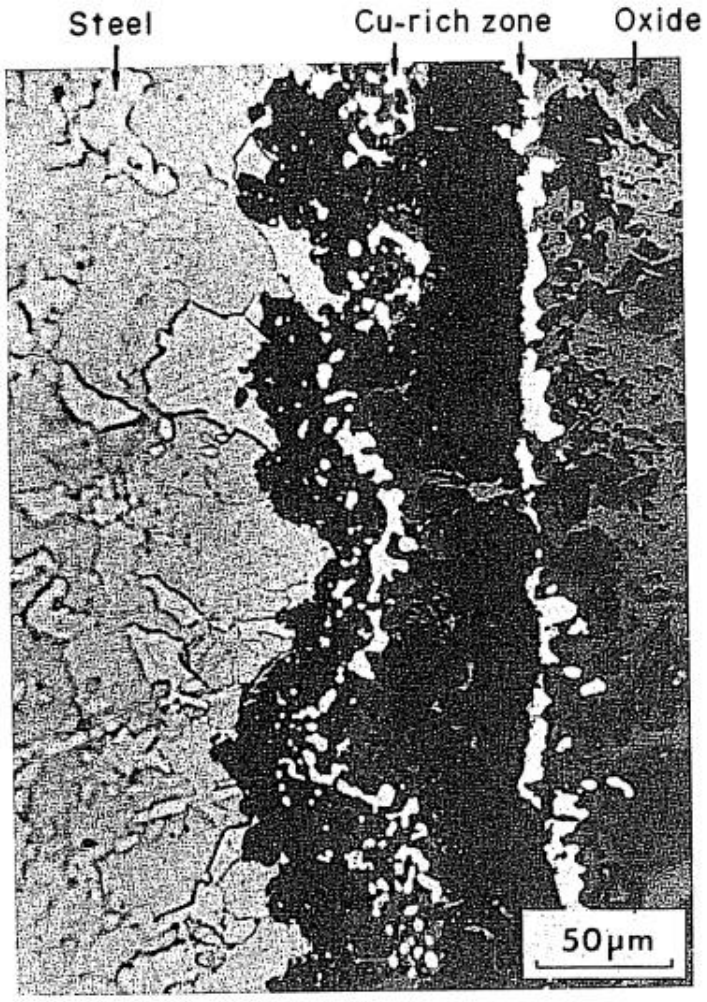

Figure 2.12. Copper-enriched zone between oxide and base metal in the steel held at 900°C for 24h [7]

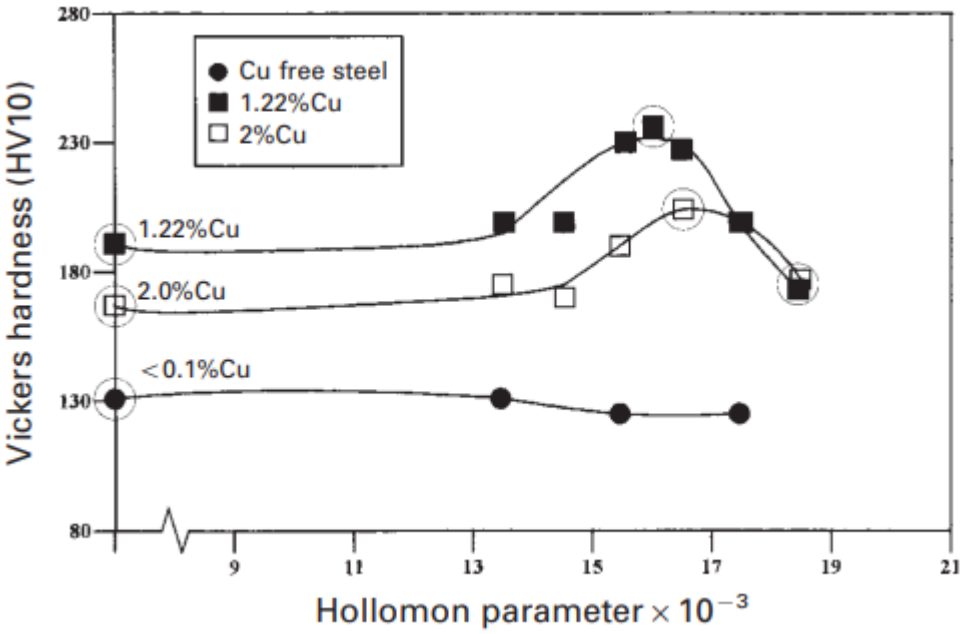

Figure 2.13. Age hardening behavior of Cu containing steels [10]

If copper containing steel age hardened, copper-rich precipitates (10-50 nm in size) may form in ferrite phase. These precipitates impede dislocation movement and thus they harden the material or retard softening as shown in Figure 2.13[10,19].

Unlike carbides and oxides that are used to strengthen steels, copper precipitates are softer than matrix phase. This allows dislocations to cut copper precipitates easily and further plastic work in the material during deformation instead of the stress concentration associated with dislocation pile-ups as in the case of carbides and oxides. Therefore, copper precipitates increase strength without losing toughness. Even some cases it increases toughness too [3,10,19].

CHAPTER 3

EXPERIMENTAL PROCEDURE

3.1 Test Specimen

To observe effects of copper on bainitic transformations and aging in 0.8%C steels, the steel alloy with the composition given in table 3.1 was prepared. In addition, the Cu: Ni ratio was kept at 2:1 to avoid copper segregation and local melting. The steel was cast into a metal mold having dimensions 25x12x2.5cm (Figure 3.1).

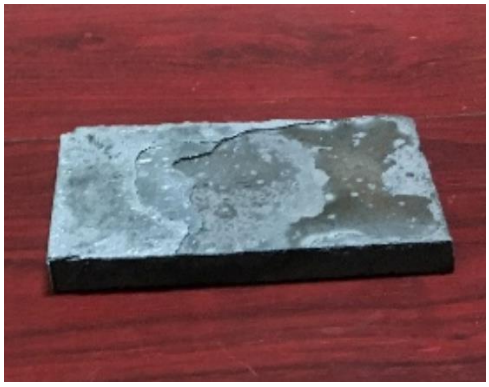

Figure 3.1. The specimen obtained after casting

"Optical Emission Spectrometer WAS Foundarymaster" in METU foundary lab was used for analysing the chemical composition of the steel plate.

Table 3.1 The chemical composition of the plate specimen.

Element	Fe	C	Si	Mn	P	S	Cr	Ni	Co	Cu	V	W	Sb
Mean Wt. %	95	0.804	0.277	0.797	0.0269	0.0377	0.0268	0.965	0.0115	1.88	0.0087	0.111	0.0264

3.2 Heat Treatment Procedure

3.2.1 Heat Treatment Equipment

MSE muffle furnace was used for austenitization and aging. The high-precision Protherm PC442T thermocouple located very close to the specimens was used for temperature measurements in austenitization and aging. A salt bath possessing a 8.5 L nitrate-nitrite mixture was used for the isothermal heat treatment of specimens.

3.2.2 Heat Treatment Parameters

Initially, the cast plate was homogenized at 1150°C for 5 hours.

The obtained results from Optical Emission Spectroscopy were uploaded to JMatPro software to calculate the TTT and CCT curves. Austenite grain size was assumed as 9 in ASTM scale. After calculating TTT and CCT curves as shown in Figure 3.2, the heat treatment temperatures and times were determined.

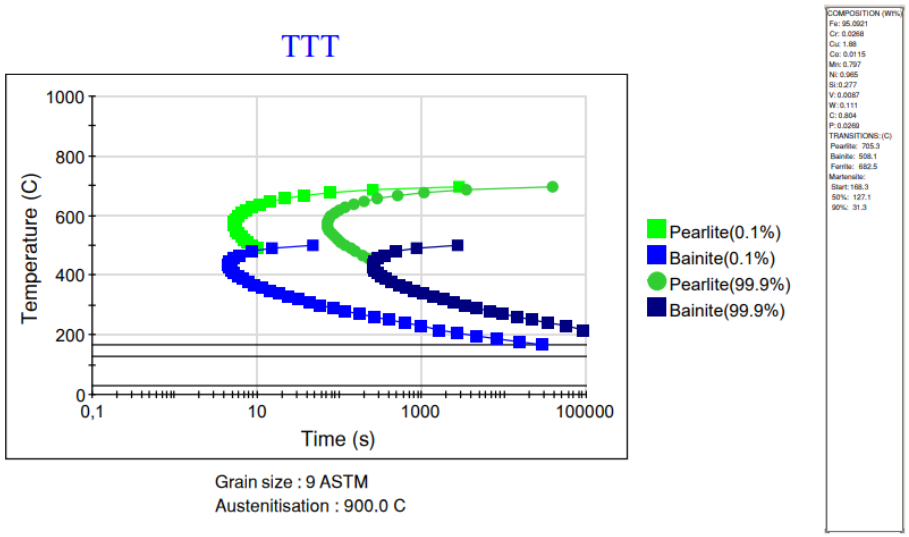

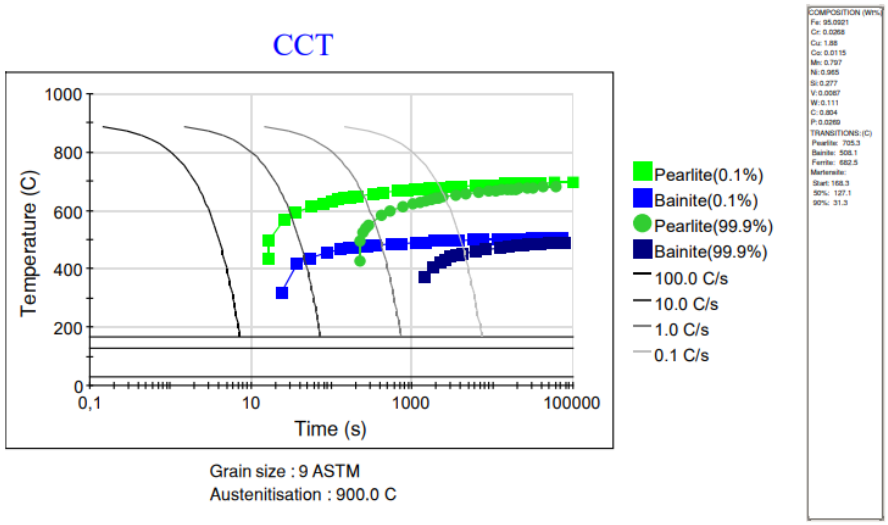

Figure 3.2. TTT and CCT curves calculated by using JMatPro software

After homogenization of the cast specimen, it was cut into 2.5 cm thick square shaped specimens. All cut samples were subjected to austenitization at 900°C for 30 minutes. The austenitization time was started after samples were reached 900°C. The temperatures of the specimens were measured by using thermocouple directly in contact with the samples. After austenitization, one sample directly quenched to oil at room temperature to obtain martensite. Other samples were subjected to isothermal heat treatment at either 170, 220, 270, 320 or 370°C to obtain bainite with various morphologies. After isothermal treatment is finished, the specimens were quenched to oil at room temperature. Finally, for ageing the samples were put in muffle furnace and kept at 450°C and 500°C for various durations. Finally, aged specimens were air cooled. The heat treatment procedure was shown schematically in Figure 3.3.

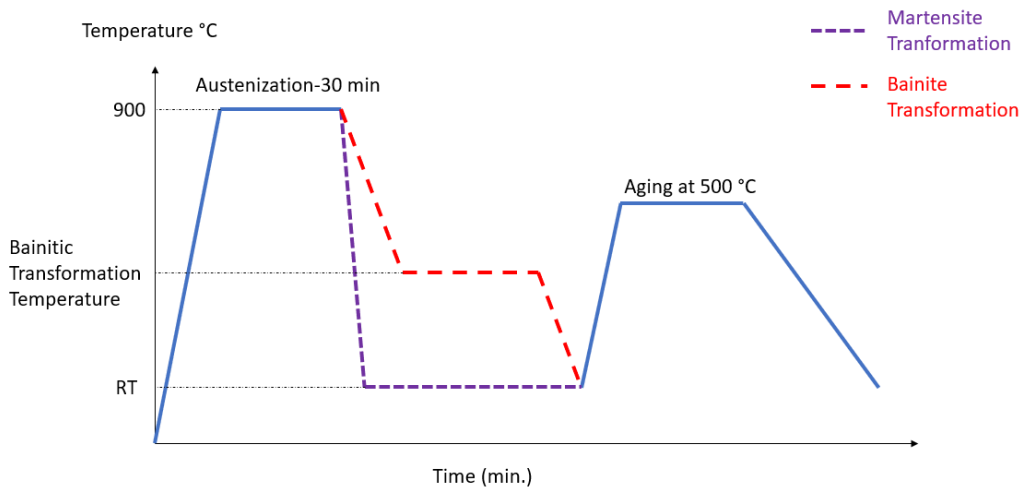

Figure 3.3.Summary of Heat Treatment Route

3.2.3 Microstructural Characterization

Specimens were prepared for optical microscopy analysis in accordance with ASTM E3 [30]. To achieve this, specimens were cut using Metkon Metacut 251 Abrasive Cutter. Metkon Ecopress 100 was used to mount the specimen into the phenolic resin. After mounting the specimens, they were ground with 180,320, 600, 1200, and 2500 grit emery papers respectively, and polished by using Mecapol P230 Polisher using 6μm and 1μm Metkon Diapat-P water-based diamond solutions.

To examine the microstructure, specimens were etched with 2% Nital solution for 1-6 seconds.

Nikon E200 Eclipse optical microscope and Clemex Vision Lite software were used for metallographic examination. Moreover, Zeiss Evo 10 SEM was used to examine the specimens at higher magnifications. Sticky copper strips were used to avoid charging during SEM examinations.

3.2.4 Hardness Measurements

To characterize bainitic transformations at various temperatures and aging for various durations Emco Universal Digital Hardness Testing Machine was used and hardnesses were taken at HV30. The specimens were mounted in phenolic resin and then ground and polished to obtain more accurate results. As very close indentations are detrimental for precision of results due to strain hardening at the vicinity of indentations, the distance minimum 2.5 times of diagonal length of previous indentation was left between indentations [31].

3.2.5 Retained Austenite Measurements with XRD

After bainitic transformations, amount of retained austenite was measured from electropolished specimens in accordance with ASTM E 975 by using GNR Arex-D. In this device, Molybdenum X-ray anode was used, and only integrated intensities of austenite and ferrite peaks were measured.

CHAPTER 4

RESULTS and DISCUSSION

4.1 Results of JMatPro TTT and CCT Simulations

For designing the bainitic and martensitic transformation heat treatments, the calculated TTT and CCT diagrams by JMatPro software were used. The calculated diagrams are given in Figure 4.1 and Figure 4.2. Martensite start temperature (Ms) was calculated as 169.3℃ by using the calculated TTT diagram, isothermal heat treatment temperatures and durations were determined as indicated in Table 4.1. In the determination of heat treatment parameters Martensite start temperature (Ms) temperature, Bainite start temperature (Bs) and the time required to obtain full bainitic transformation (according to the diagrams) were considered. Moreover, TTA diagram was also simulated as given in Figure 4.3 to determine austenitization temperature and its duration. After examination of the TTA diagram, the austenitization is carried out at 900°C for 30 minutes to ensure full austenitization.

Following the isothermal heat treatments, specimens were aged at 450℃ and 500℃ for various durations. The aging temperatures were determined by considering work of Fourlaris et al. [35] and Uzer [36]. The aging parameters were given in Table 4.2.

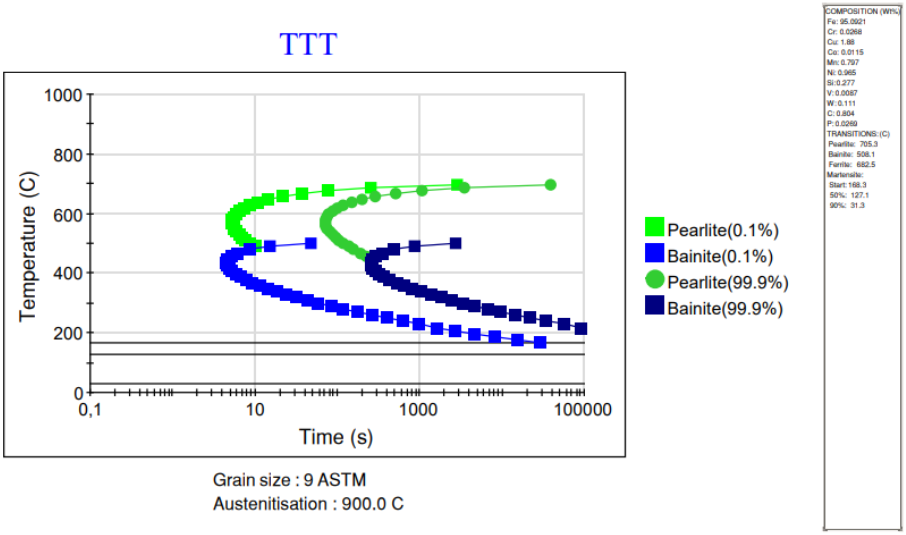

Figure 4.1. Calculated TTT diagram of the alloy.

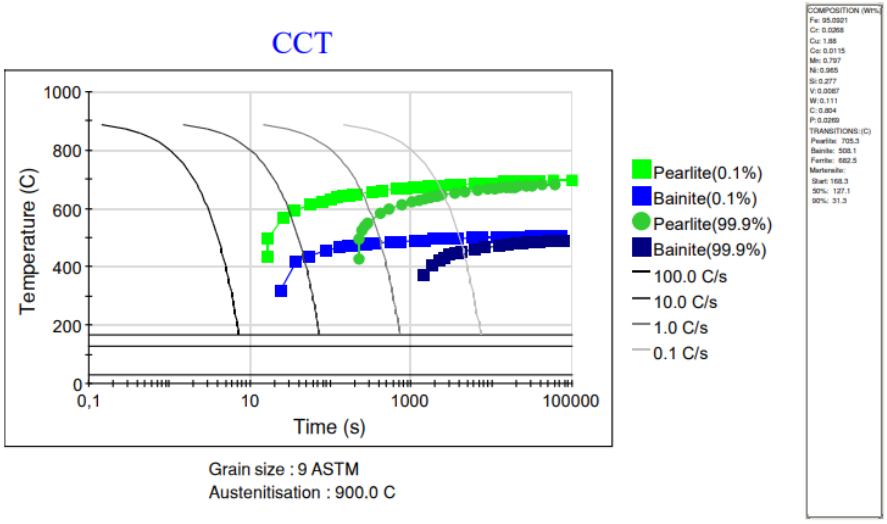

Figure 4.2. Calculated CCT diagram of the alloy.

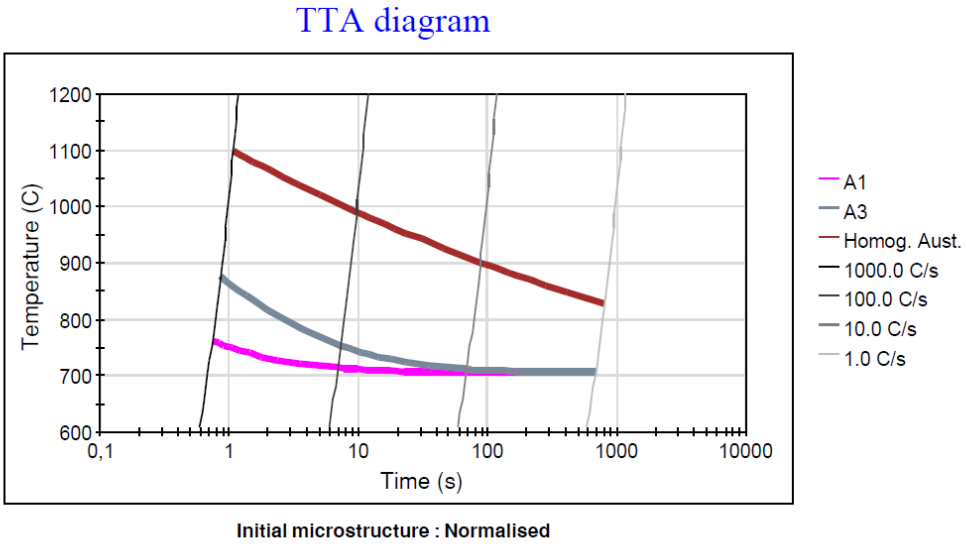

Figure 4.3. Calculated TTA diagram of the Specimen

Table 4.1 Isothermal heat treatment temperatures and durations depending on the calculated TTT diagram.

Austenitization Temperature (°C)	**Applied Heat Treatment**	**Heat Treatment Temperature (°C)**	**Duration (hr.)**
900	Quenching	-	-
	Bainitic Transformation	170 (Just above Ms)	40
		220	25
		270	3
		320	1
		370	0.30

Table 4.2 The parameters of the ageing performed after isothermal heat treatment

Applied Heat Treatment	**Isothermal Heat-Treatment Temperature (°C)**	**Duration (hr.)**	**Duration of Aging At 450°C (min.)**	**Duration of Aging At 500°C (min.)**
Quenching	-	-	-	0,30,60 and 120
Bainitic Transformation	170 (Just above Ms)	40	-	
	220	25	-	
	270	3	0,10,60,90, 180,270 and 360	
	320	1		
	370	0.30		

4.2 Optical Microscope Images of Aged and Unaged Specimens

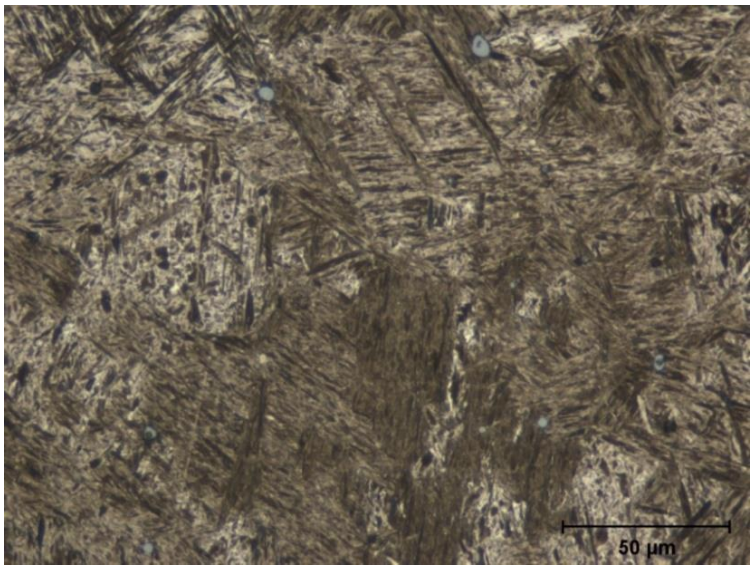

Figure 4.4. Optical Micrograph of Quenched Specimen. Martensitic structure.

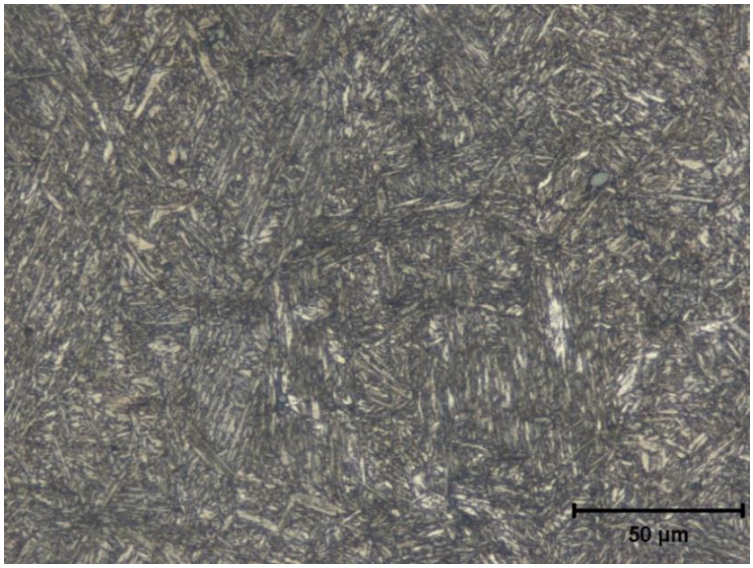

Figure 4.5. Optical Micrograph of the specimen after quenching and aging at 500℃ for 2-hours. Tempered Martensite.

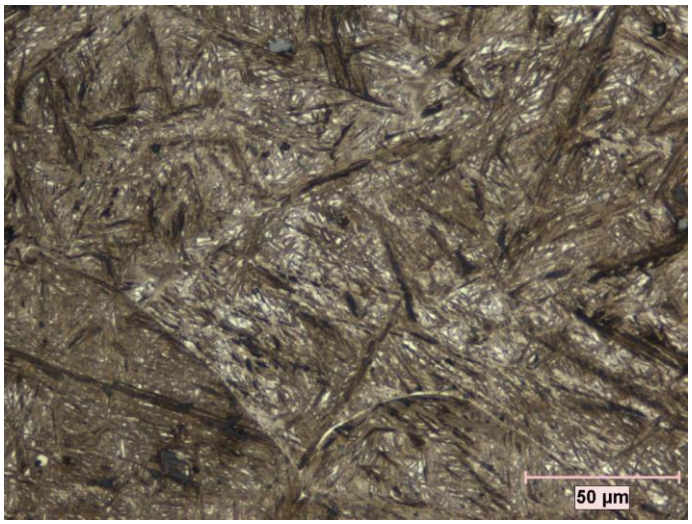

Figure 4.6. Optical Micrograph of Isothermally Heat-Treated Specimen at 170℃ for 41 hours. The microstructure seems to be mostly bainite. There are small white areas which are most probably M/A islands.

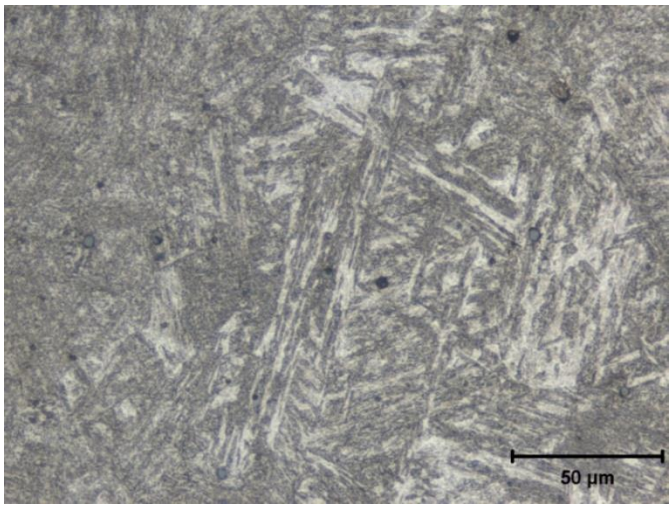

Figure 4.7. Optical Micrograph of Isothermally Heat-Treated specimen at 170℃ for 41 hours. Then aged at 500 C for 2-hours. The microstructure seems to be mostly bainite.

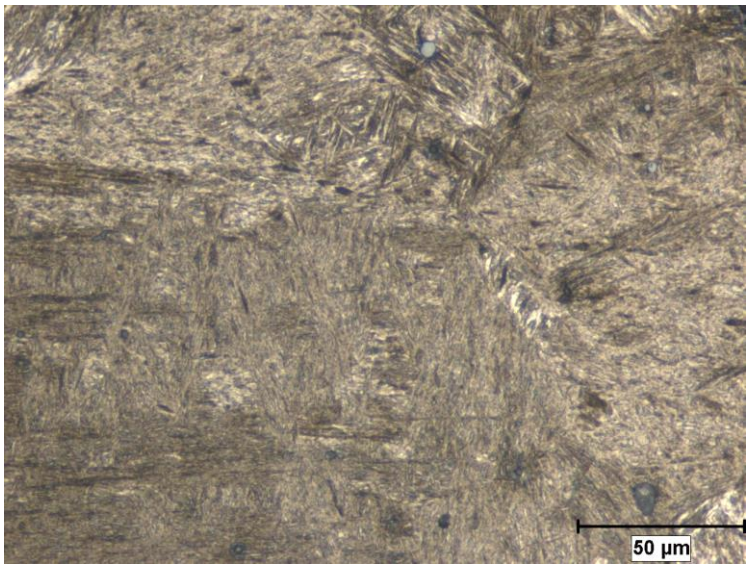

Figure 4.8. Optical Micrograph of Isothermally Heat-Treated Specimen at 220℃ for 25 hours. The microstructure seems to be mostly bainite. A few amounts of M/A islands are seen.

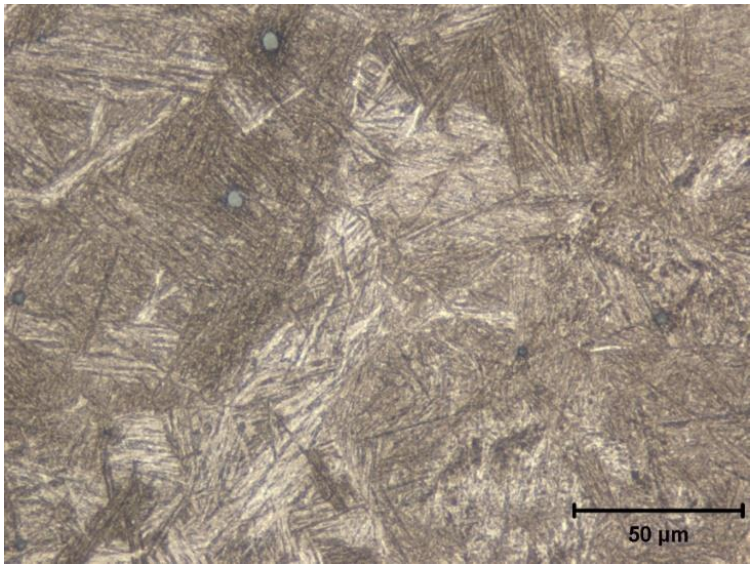

Figure 4.9. Optical Micrograph of Isothermally Heat-Treated at 220℃ for 25 hours and then aged at 500 C for 2 hours.

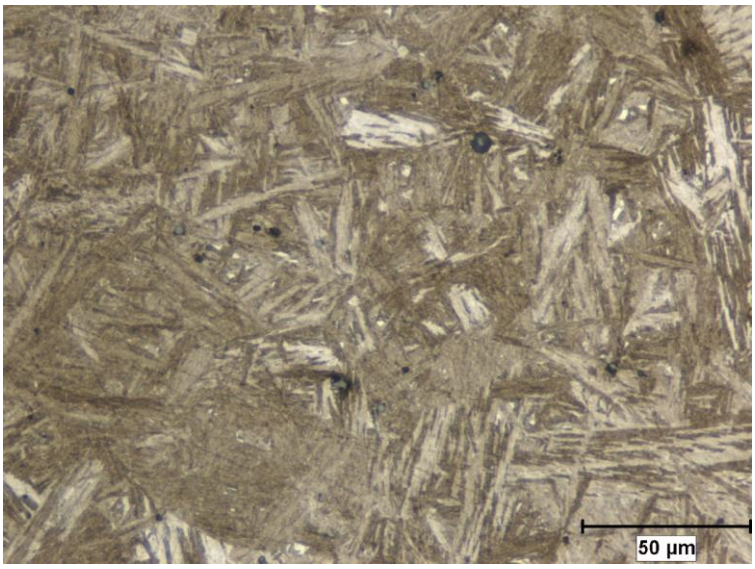

Figure 4.10. Optical Micrograph of Isothermally Heat-Treated Specimen at 270℃ for 3 hours. The microstructure seems to be mostly bainite.

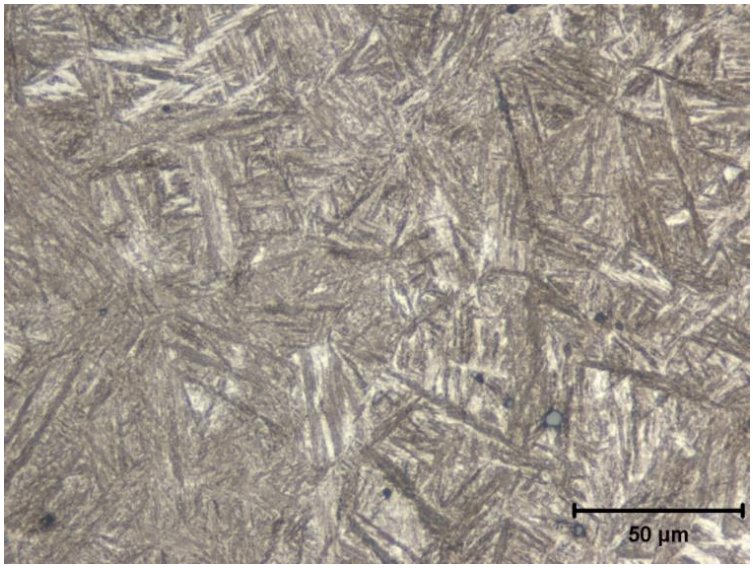

Figure 4.11. Optical Micrograph of Isothermally Heat-Treated at 270℃ for 3 hours. Then aged at 500 C for 2-hours.

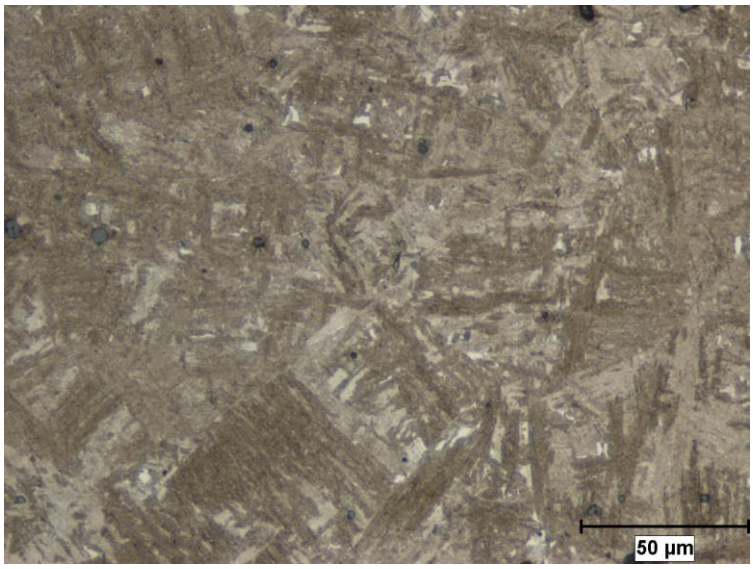

Figure 4.12. Optical Micrograph of Isothermally Heat-Treated Specimen at 320℃ for 1 hour. The microstructure seems to be mostly bainite. There are a few light-colored areas which are most probably belong to M/A islands.

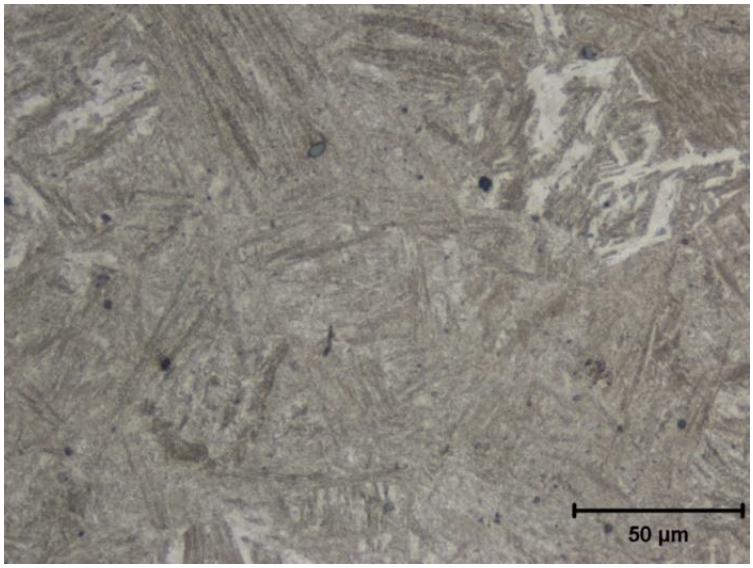

Figure 4.13. Optical Micrograph of Isothermally Heat-Treated at 320℃ for 1 hours. Then aged at 500 C for 2-hours.

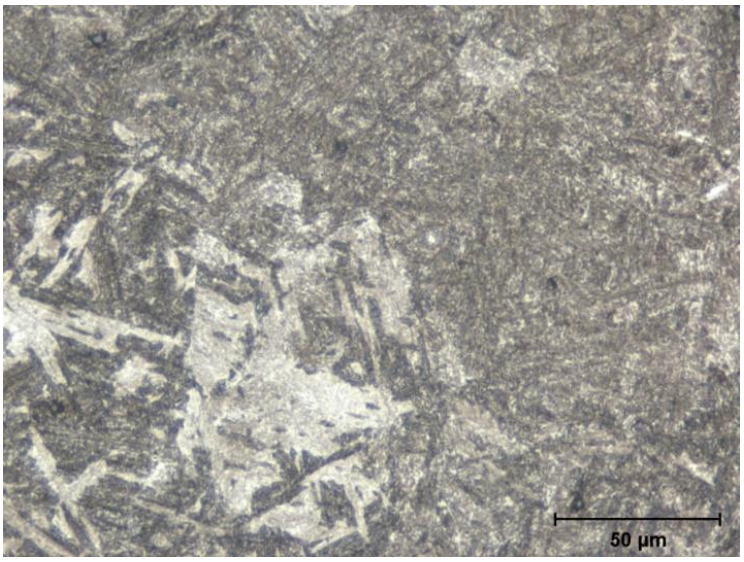

Figure 4.14. Optical Micrograph of Isothermally Heat-Treated Specimen at 370℃ for 0.30 hour. The microstructure seems to be mostly bainite. There are light colored areas which are most probably belong to M/A islands.

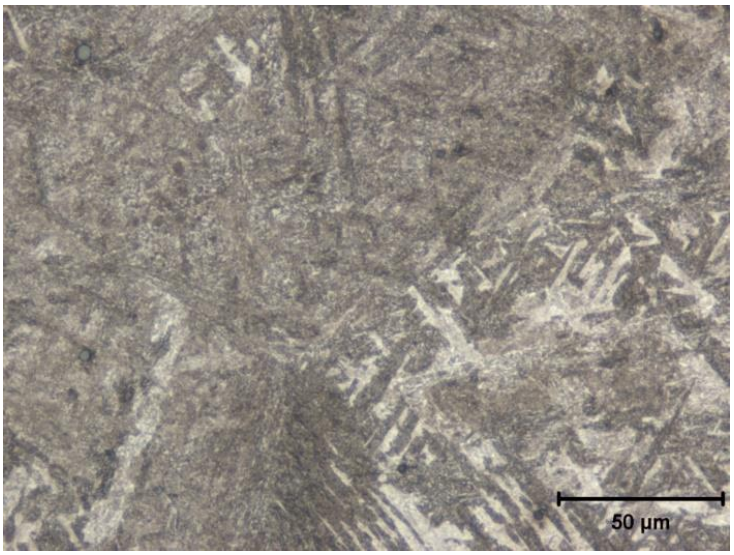

Figure 4.15. Optical Micrograph of Isothermally Heat-Treated at 370℃ for 0.30 hour. Then aged at 500℃ for 2-hours. The microstructure seems to be mostly bainite.

Quenched Specimens

As seen in Figure 4.4, the microstructure of as-quenched specimen consists of martensite. Though cannot be resolved, some amount of retained austenite is expected. In accordance with the carbon content, martensite needles are in plate morphology.

When the quenched specimen is aged, martensite plates become rounded (Figure 4.5). As a result of the aging, the microstructure has transformed into tempered martensite.

Isothermally Heat-Treated Specimen at 170℃

The micrograph of the isothermally treated specimen at 170℃ Figure 4.7show that bainitic transformation is nearly complete (Figure 4.6). Acicular bainite sheaves are seen. A few white areas are present, which are most probably the M/A regions (either retained austenite or martensite).

According to optical microscopic examinations, after aging the bainite sheaves become more visible. This might be due to fine carbide precipitation at the sheave boundaries. The light-colored needles in Figure 4.7 may belong to M/A regions. However, their morphology is different from the classical appearance of M/A. Therefore, needs SEM study.

Isothermally Heat-Treated Specimen at 220℃

Similar to that of previous heat treatment, an isothermal treatment at 220℃, the microstructure seems to be mostly bainite (Figure 4.8). A noticeable change could not be seen in comparison to treatment at 170℃ (Figure 4.6).

After aging treatment, the bainite sheaves become more visible (Figure 4.9).

Isothermally Heat-Treated Specimen at 270℃

Similar to previous heat treatment, the specimen treated at 270℃ for 3 hours yielded bainitic microstructure. However, the bainite sheaves are thicker than the low-temperature treatments (Figure 4.10).

After aging, like in previous specimens, the bainite sheaves become more visible (Figure 4.11)

Isothermally Heat-Treated Specimen at 320℃

The specimen treated at 320℃ for 3 hours yielded bainitic microstructure. Like the sample treated at 270℃, the bainite sheaves are thick (Figure 4.12).

After aging, similar to previous specimens, the bainite sheaves become more visible (Figure 4.13).

Isothermally Heat-Treated Specimen at 370℃

Similar to previous heat treatment, the isothermally treated specimen at 370℃ exhibits a coarse bainitic structure (Figure 4.14). The light-appearing and dark-appearing bainite sheaves are very evident in this specimen. The different contrasted sheaves may be because the light-appearing regions belong to the bainite that transformed at the early stages of the isothermal treatment.

Aging at 500℃ did not change the microstructure (Figure 4.15).

4.3 SEM Study of Aged and Unaged Specimens

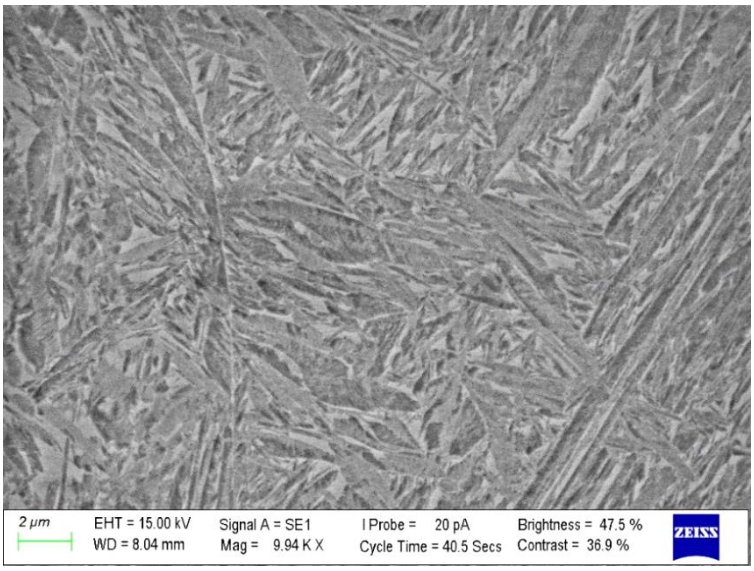

Figure 4.16. SEM micrograph of the Quenched Specimen. Martensite.

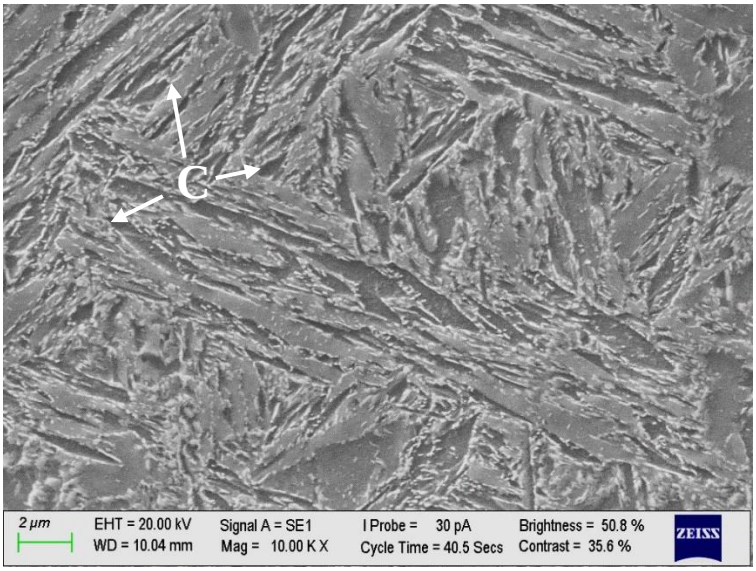

Figure 4.17. SEM micrograph of the specimen after quenching and 2-hour ageing. A light-colored fine precipitation is seen at the boundaries which are most probably cementite (shown as “C”).

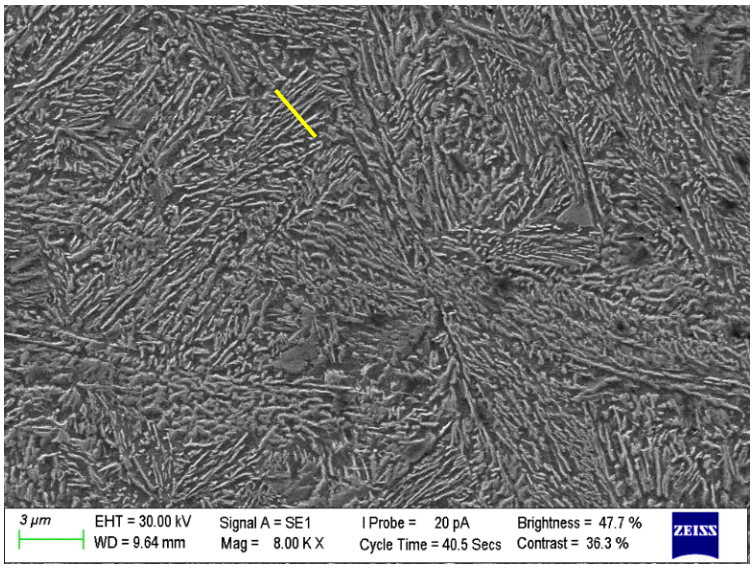

Figure 4.18. SEM image of Isothermally Heat-Treated at 170℃ for 41 hours. Mostly bainitic structure with carbide precipitation. Bainite sub-unit width is approximately 0.2 µm.

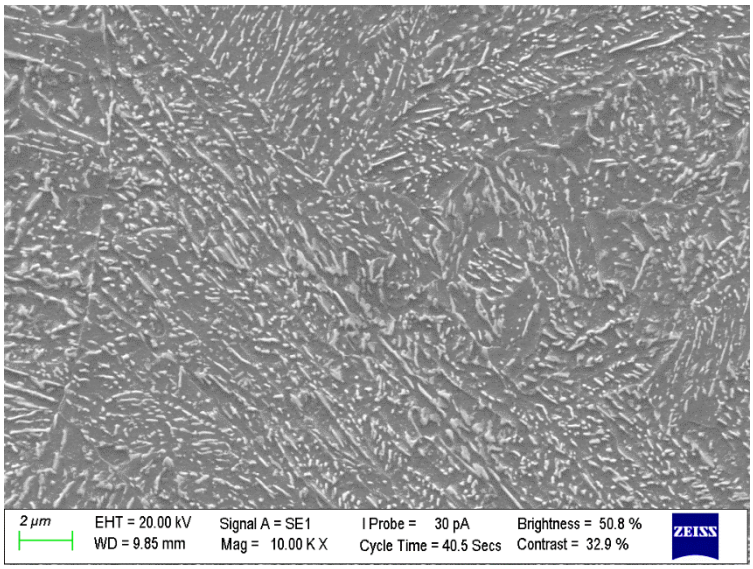

Figure 4.19. SEM image of Isothermally Heat-Treated at 170℃ for 41 hours and then aged 2-hours. The carbides appear as rounded, light contrasted particles. The carbides seem to become rounded after the ageing process.

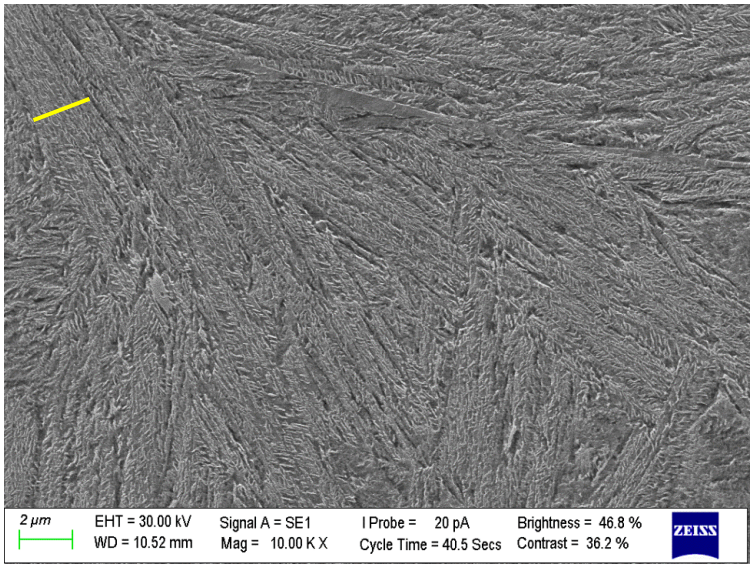

(a)

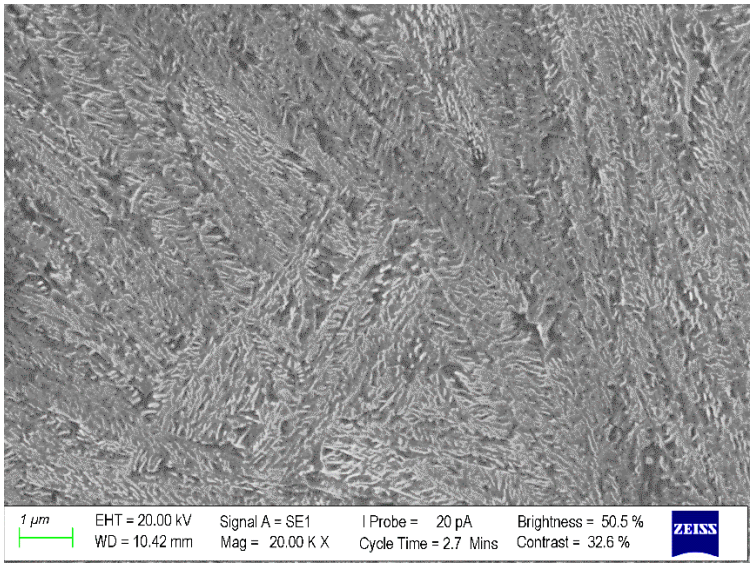

(b)

Figure 4.20. (a) SEM image of Isothermally Heat-Treated at 220°C for 25 hours. Mostly bainitic structure with carbide precipitation. Bainite sub-unit width is approximately 0.2 µm. (b) At higher magnification.

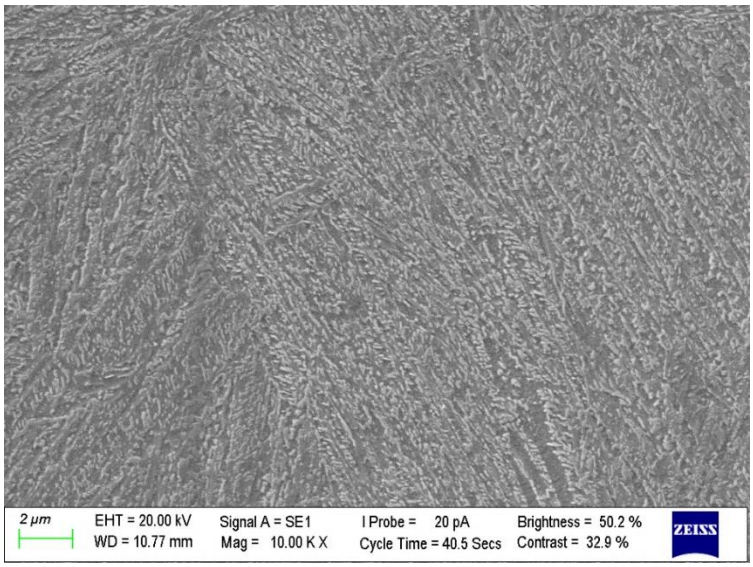

(a)

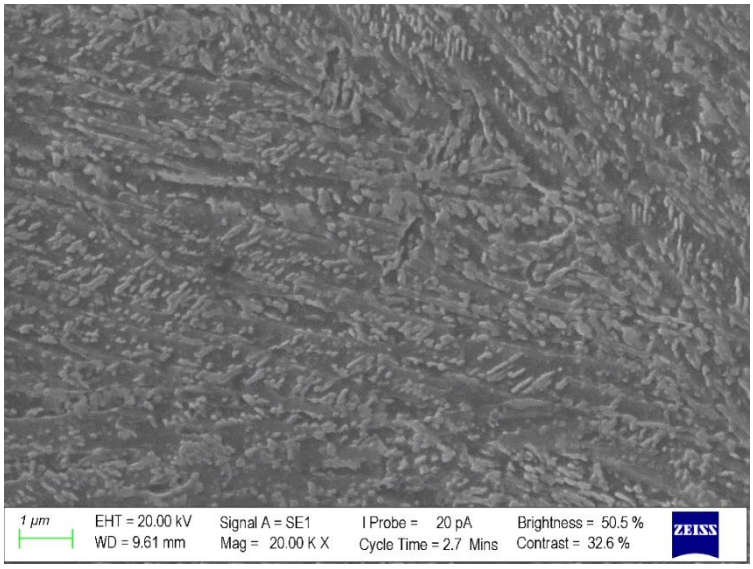

(b)

Figure 4.21. (a) SEM image of Isothermally Heat-Treated at 220℃ for 25 hours and 2-hour Aged Specimen. The carbides seem to become rounded after the ageing process. (b) At higher magnification.

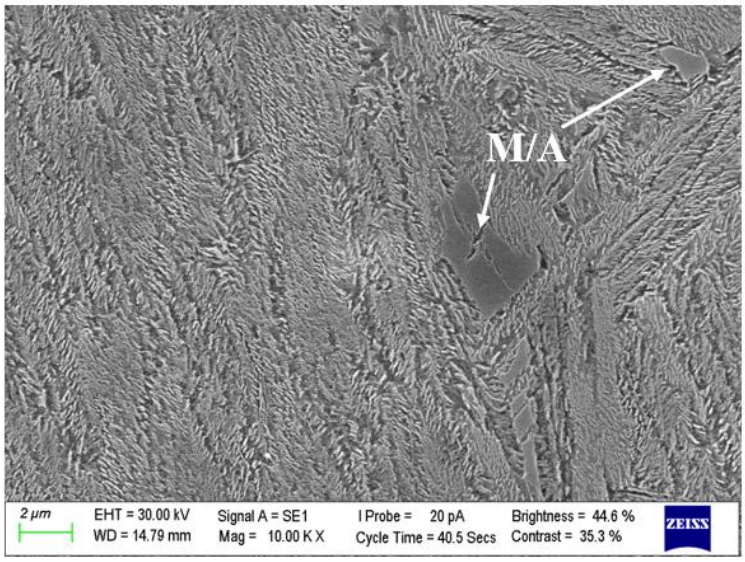

(a)

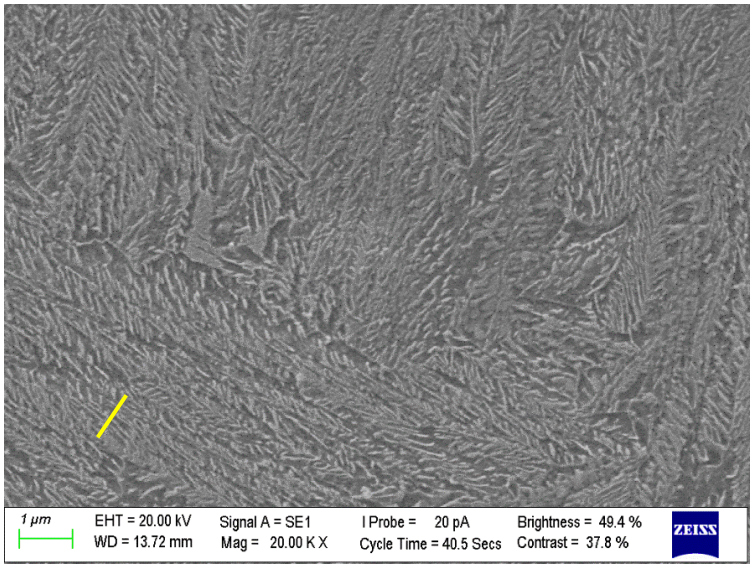

(b)

Figure 4.22. (a)SEM image of Isothermally Heat-Treated at 270℃ for 3 hours. Mostly bainitic structure with carbide precipitation. Also, small Martensite/Austenite islands(M/A) were seen. (b) At higher magnification. Bainite sub-unit width is approximately 0.2 μm.

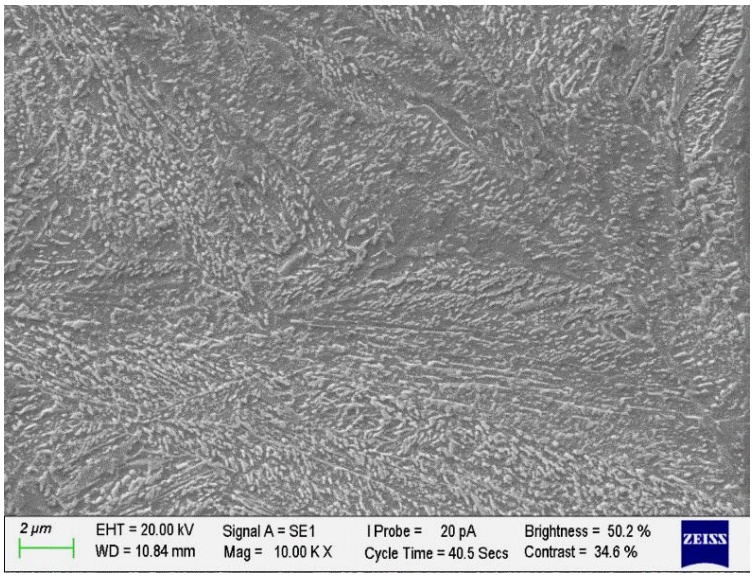

(a)

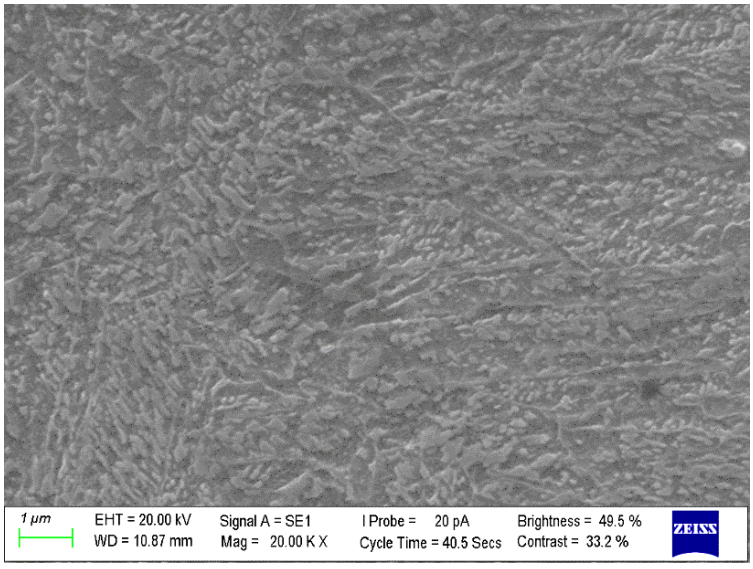

(b)

Figure 4.23. (a) SEM image of Isothermally Heat-Treated at 270°C for 3 hours and 2-hour Aged Specimen. The carbides seem to become rounded after the ageing process. (b) At higher magnification.

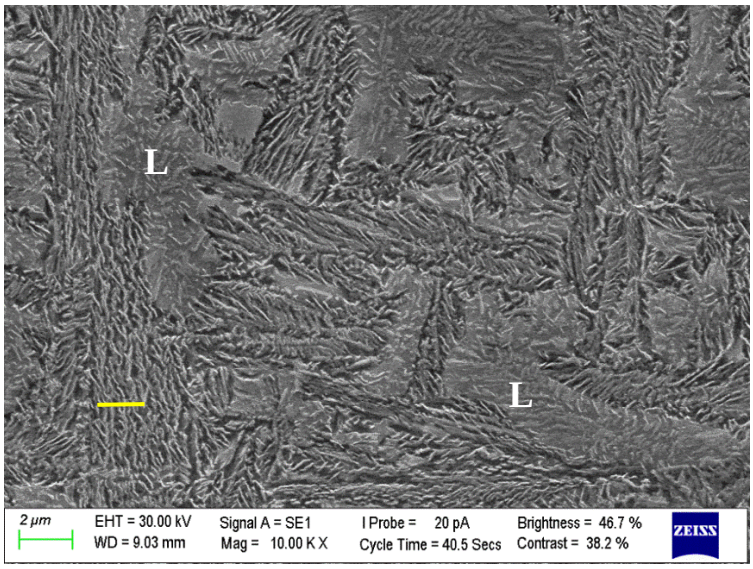

(a)

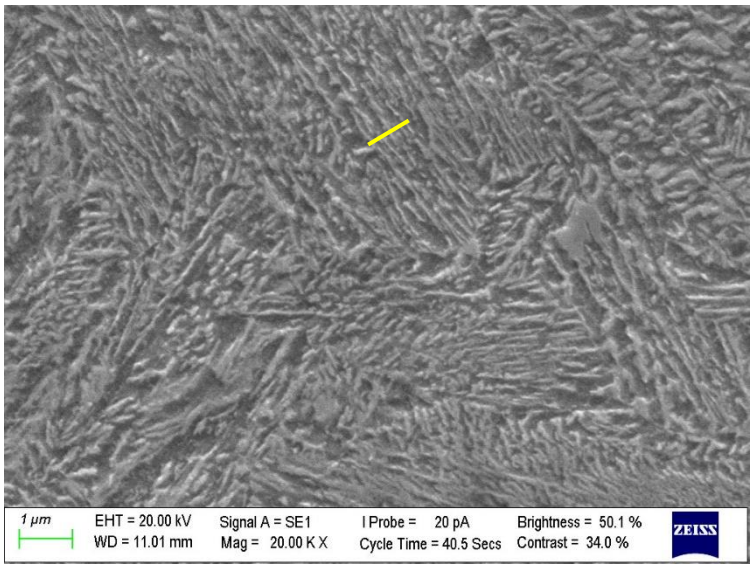

(b)

Figure 4.24.(a) SEM image of Isothermally Heat-Treated at 320℃ for 1 hours. Mostly bainitic structure with carbide precipitation. Bainite sub-unit width is approximately 0.4 µm. There are darker regions shown with L have a slightly different color contrast than other regions but same morphology. (b) At higher magnification.

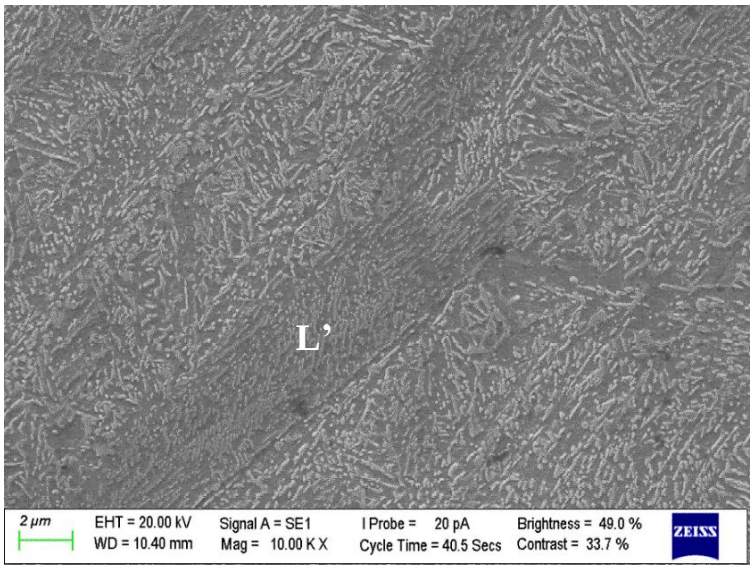

(a)

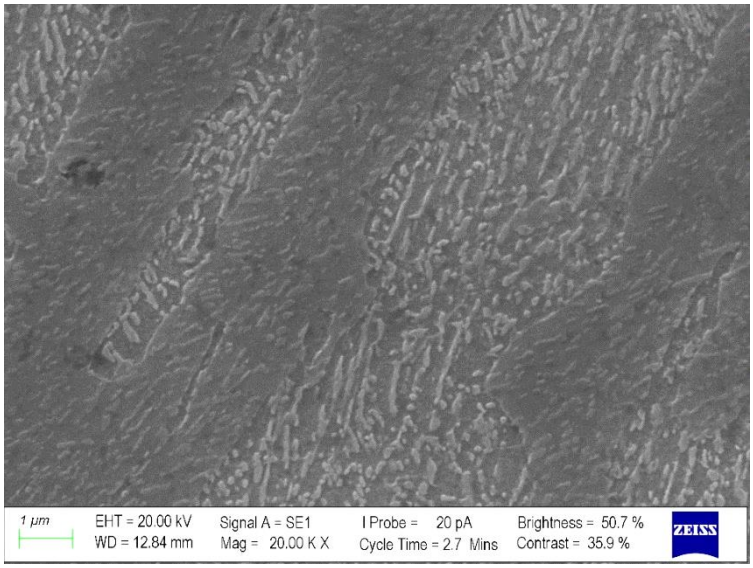

(b)

Figure 4.25. SEM image of Isothermally Heat-Treated at 320°C for 1 hours and 2-hour Aged Specimen. The carbides seem to become rounded after the aging process. There are darker regions shown L’ have a slightly different color contrast than other regions but same morphology.

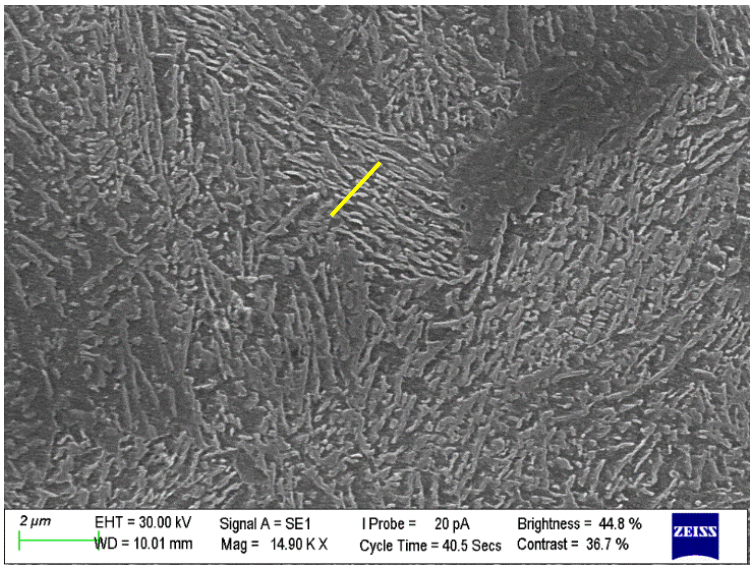

Figure 4.26. SEM image of Isothermally Heat-Treated Specimen at 370°C for 0.30 hour. Mostly bainitic structure with carbide precipitation. Bainite sub-unit width is approximately 0.4 µm.

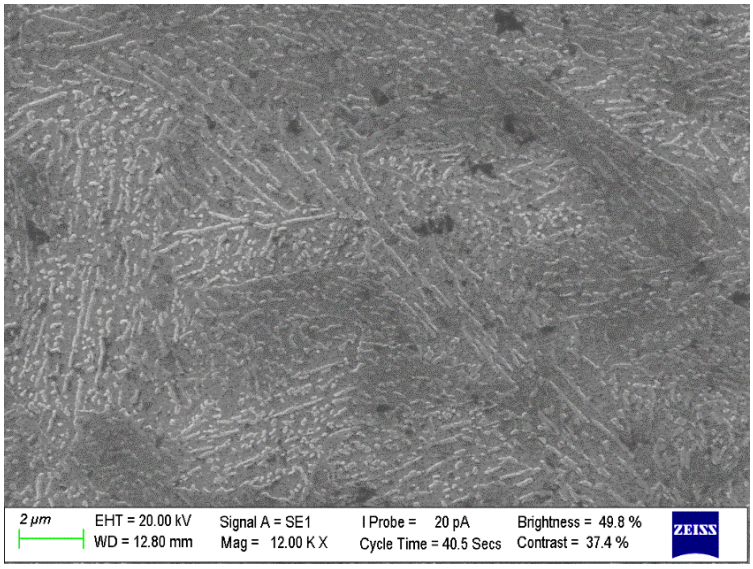

Figure 4.27. SEM image of Isothermally Heat-Treated at 370°C for 0.30 and 2-hour Aged Specimen. The carbides seem to become rounded after the ageing process.

Quenched Specimens

In Figure 4.16, it is seen that the microstructure consists of plate martensite. In Figure 4.17, it is seen that aging at 500°C (it can be assumed as tempering) caused carbide precipitation at the plate boundaries. It can be assumed that these carbides are of cementite type because cementite is stable at that temperature [16, 34].

Moreover, the difference between Figure 4.18 and Figure 4.19 shows that martensite plates are slightly rounded after aging.

Isothermally Heat-Treated Specimen at 170°C

Figure 4.18 shows the bainitic transformation at 170°C. The bainite sheaves are very narrow. According to the measurement performed on the test line (yellow bar) (Figure 4.18), the approximate bainite sub-unite size is 0.2 μm. The carbide precipitation at certain crystallographic directions is evident (Figure 4.18). This means that the amount of copper itself is insufficient to suppress the carbide precipitation.

The carbides seem to become rounded after aging, as shown in Figure 4.19. This can be explained by the thermodynamic driving force toward the reduction in interfacial energy between the carbide and ferrite phases [12].

Isothermally Heat-Treated Specimen at 220°C

Figure 4.20 shows that the bainitic transformation at 220°C is nearly complete. SEM images clearly show carbide precipitation within bainite sub-units with specific crystallographic directions. Bainite sub-unit width is approximately 0.2 μm in this specimen as well. Similar to that of previous heat treatment, carbides are slightly spheroidized after aging (Figure 4.21).

Isothermally Heat-Treated Specimen at 270°C

SEM images clearly show carbide precipitation within bainite sub-units with specific crystallographic directions. In addition, small M/A islands were seen

(Figure 4.22). Similar to that of previous heat treatment, carbides slightly spheroidized after aging. Bainite sub-unit width is approximately 0.2 μm in this specimen as well.

Isothermally Heat-Treated Specimen at 320℃

SEM images clearly show carbide precipitation within bainite sub-units with specific crystallographic directions. Bainite sub-units seem wider when Figure 4.24 compared with Figure 4.18, Figure 4.20, and Figure 4.22. Similar to that of previous heat treatment, carbides slightly spheroidized after aging. The darker appearing regions in Figure 4.24 and 4.25 shown as L and L' can belong to the bainite sheaves that formed at a different time interval than the other regions but there is no evidence at that stage.

Isothermally Heat-Treated Specimen at 370℃

Figure 4.26 shows the bainitic transformation at 370℃. Under SEM, it is seen that this temperature yields the thickest bainite sub-unit width (0.4μm). Also, carbide precipitates seem rounded when Figure 4.26 compared with previous SEM images of isothermally heat-treated specimens. Hence, the effect of aging on carbide morphology is the lowest for isothermally heat-treated samples at 370℃. Moreover, the dark contrasted regions in Figure 4.26 are believed to belong to the bainite, which forms at later stages of transformation.

Table 4.3 The Approximate Bainite Sub-Unit Widths Depending on Heat Treatment Temperature

Applied Heat Treatment	**Approximate Bainite Sub-Unit Width (**μm)
Isothermally Heat Treated at 170°C	0.2
Isothermally Heat Treated at 220°C	0.2
Isothermally Heat Treated at 270°C	0.2
Isothermally Heat Treated at 320°C	0.4
Isothermally Heat Treated at 370°C	0.4

4.4 Retained Austenite Measurements

Table 4.4 Retained Austenite Measurements Before Aging Process

Applied Heat Treatment	**Retained Austenite (%)**
Quenched	5.5± 0.1
Isothermally Heat Treated at 170°C	<1
Isothermally Heat Treated at 220°C	<1
Isothermally Heat Treated at 270°C	<1
Isothermally Heat Treated at 320°C	<1
Isothermally Heat Treated at 370°C	<1

The amount of retained austenite values obtained from XRD analysis are given in Table 4.4. Approximately 5.5% retained austenite is present in as-quenched specimen. Also, a reasonable amount of retained austenite was expected in bainitic specimens. However, retained austenite could not be detected in isothermally heat-treated specimens. This can be explained by the study of Caballero et al. [32] and SEM images. According to this study, if carbide precipitation cannot be

suppressed, retained austenite will decompose into ferrite and carbide. It seems that the Cu element alone could not suppress the carbide precipitation.

4.5 Hardness Measurements

Table 4.5 Hardness Values of Martensitic and Bainitic Specimens Before Aging

Specimen	**HV30**
Quenched	652±22
Isothermally Heat Treated at 170°C	661±10
Isothermally Heat Treated at 220°C	630±13
Isothermally Heat Treated at 270°C	532±13
Isothermally Heat Treated at 320°C	475±4
Isothermally Heat Treated at 370°C	405±6

Hardness values of both the bainitic and martensitic specimens are given in Table 4.5. It can be seen that highest hardness values were obtained from as-quenched and isothermally heat-treated specimens at 170°C. It is expected for the as-quenched specimen to yield the highest hardness value. However, a similar hardness value achieved by isothermally heat-treated specimen at 170°C indicates that a bainitic structure formed at a substantially low temperature (i.e., close to Ms) can reach to that of as-quenched specimen. The high hardness value in isothermally heat-treated specimen at 170°C cannot be attributed to incomplete bainitic transformation and presence of high amount of martensite. If this was the case, some amount of retained austenite should be observed in 170°C bainitic specimen as well.

It is observed that when the isothermal heat treatment temperatures increase, hardness values decrease. The hardness of specimen isothermally treated at 170°C yields 661HV. However, the hardness drops gradually as the isothermal transformation temperature increases from 170°C to 370°C. The specimen treated at 370°C yields only 405 HV. This can be attributed to the bainitic sub-unit width which become thicker at high transformation temperatures as shown in Table 4.3 (3,37). Also, the bainitic transformation may not be complete and some amount of martensite may form in the microstructure in the form of M/A and effect the hardness value. However, such a high amount of M/A was not observed in the microstructure.

4.5.1 Effect of Aging Time and Temperatures on Hardness Values of Martensitic and Bainitic Specimens

Table 4.6 Hardness measurements with HV30 scale after aging at 500°C

Isothermal Heat Treatment Temperature	Hardness (HV30) at Aging Time(min.)			
	0	30	60	120
Quench	651±22	476±1	424±7	403±2
170°C	661±10	468±1	439±3	409±2
220°C	630±12	461±3	429±1	406±5
270°C	532±13	435±12	412±4	398±2
320°C	475±4	425±4	378±4	391±5
370°C	405±6	408±1	376±6	384±6

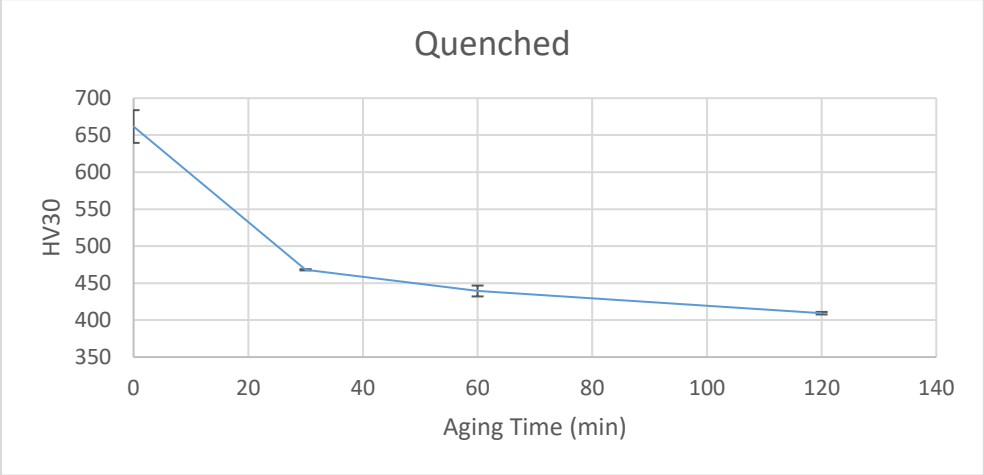

Figure 4.28. Ageing Time vs. Hardness Graph of Quenched Specimen (Aged at 500°C)

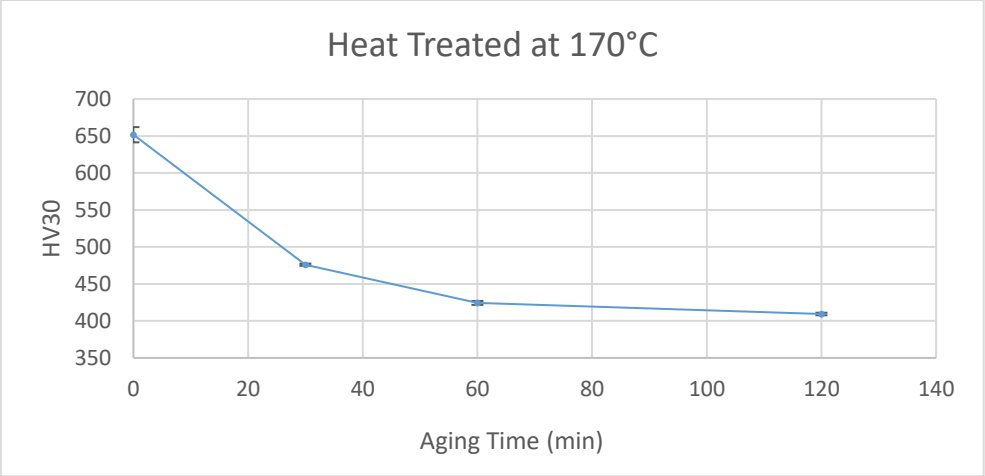

Figure 4.29. Aging Time vs. Hardness Graph of Isothermally Heat-Treated Specimen at 170°C (Aged at 500°C)

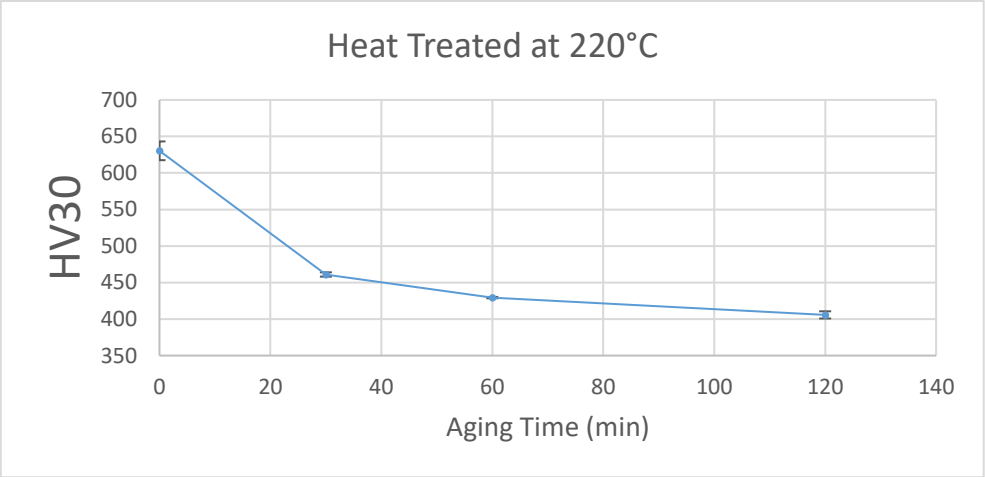

Figure 4.30. Aging Time vs. Hardness Graph of Isothermally Heat-Treated Specimen at 220°C (Aged at 500°C)

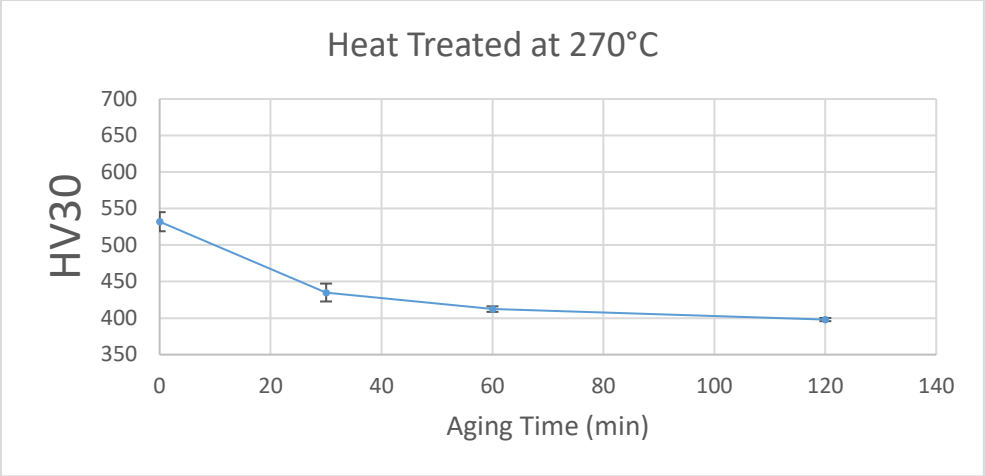

Figure 4.31. Aging Time vs. Hardness Graph of Isothermally Heat-Treated Specimen at 270°C (Aged at 500°C)

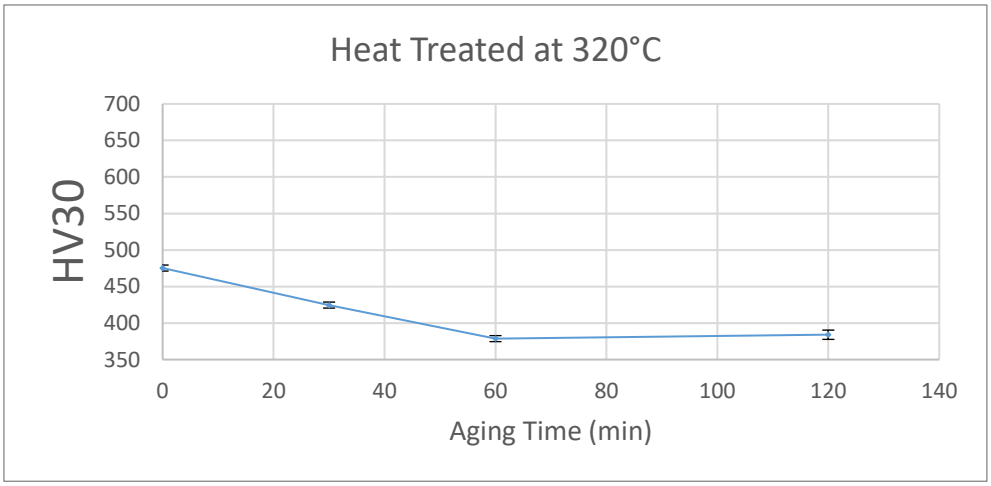

Figure 4.32. Aging Time vs. Hardness Graph of Isothermally Heat-Treated Specimen at 320°C (Aged at 500°C)

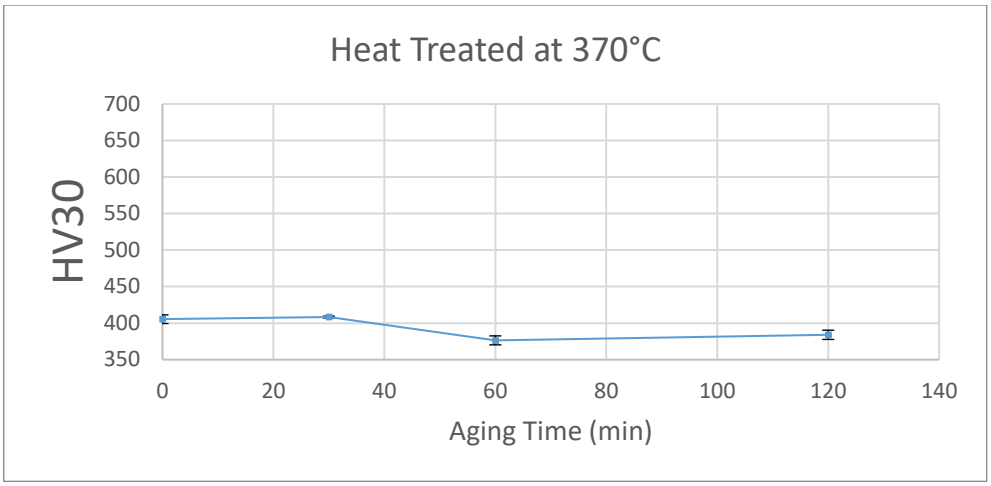

Figure 4.33. Aging Time vs. Hardness Graph of Isothermally Heat-Treated Specimen at 370°C (Aged at 500°C)

Table 4.7 Hardness Results Obtained from the Specimens Aged at 450°C

Isothermal Heat Treatment Temperature	Hardness (HV30) at Aging Time(min.)						
	0	10	60	90	180	270	360
270°C	565±2	450±2	435±2	417±1	417±3	393±4	390±3
320°C	482±2	421±4	413±2	409±2	396±6	391±4	372±3
370°C	385±1	379±2	382±2	380±1	404±4	369±1	374±4

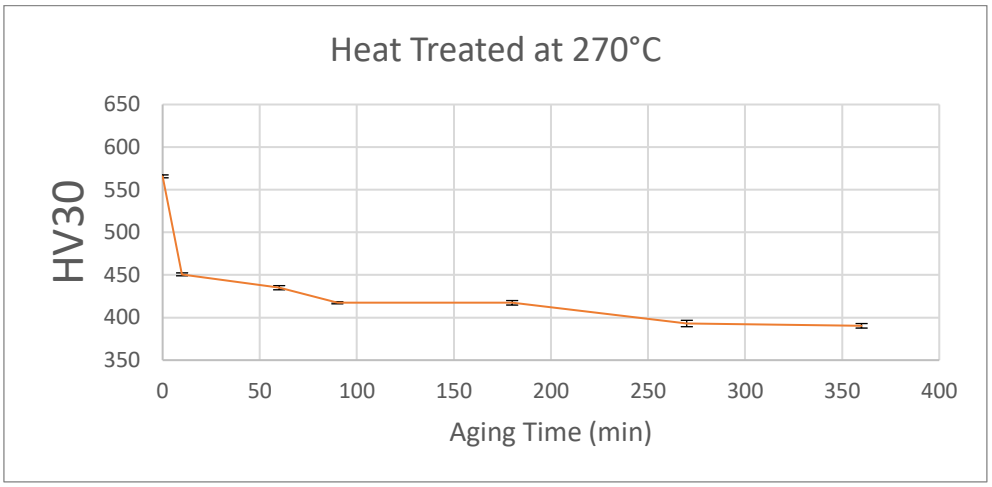

Figure 4.34. Aging Time vs. Hardness Graph of Isothermally Heat-Treated Specimen at 270°C (Aged at 450°C)

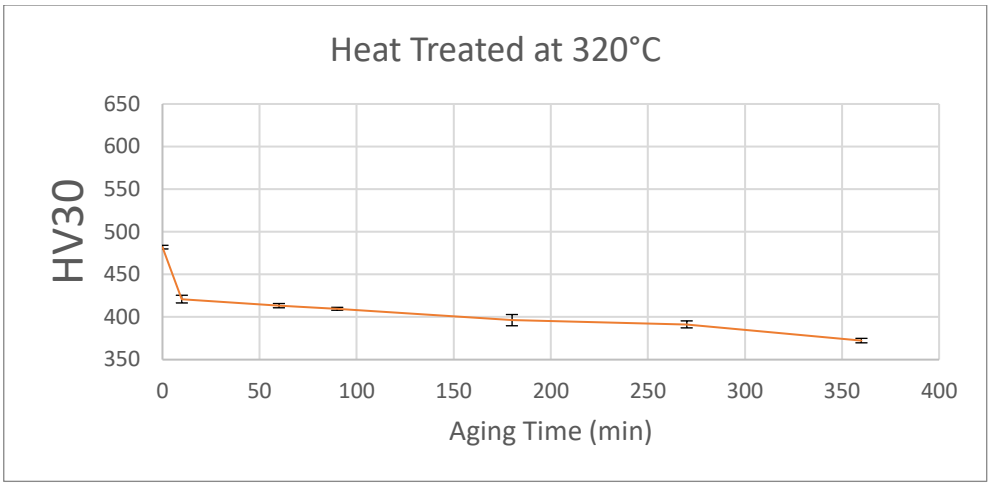

Figure 4.35 Aging Time vs. Hardness Graph of Isothermally Heat-Treated Specimen at 320°C (Aged at 450°C)

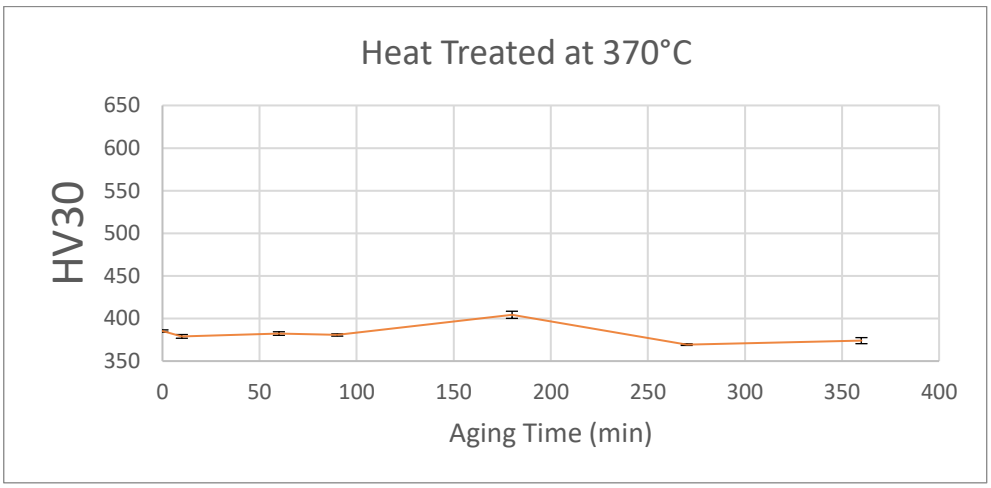

Figure 4.36. Aging Time vs. Hardness Graph of Isothermally Heat-Treated Specimen at 370°C (Aged at 450°C)

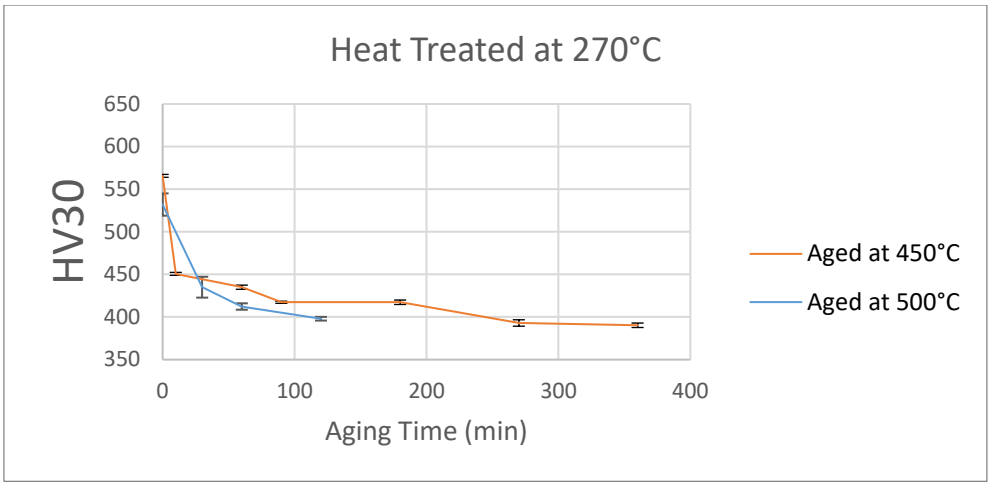

Figure 4.37.Superposition of Aging Time vs. Hardness Graphs of Isothermally Heat-Treated Specimens at 270°C, then aged at 450°C & 500°C

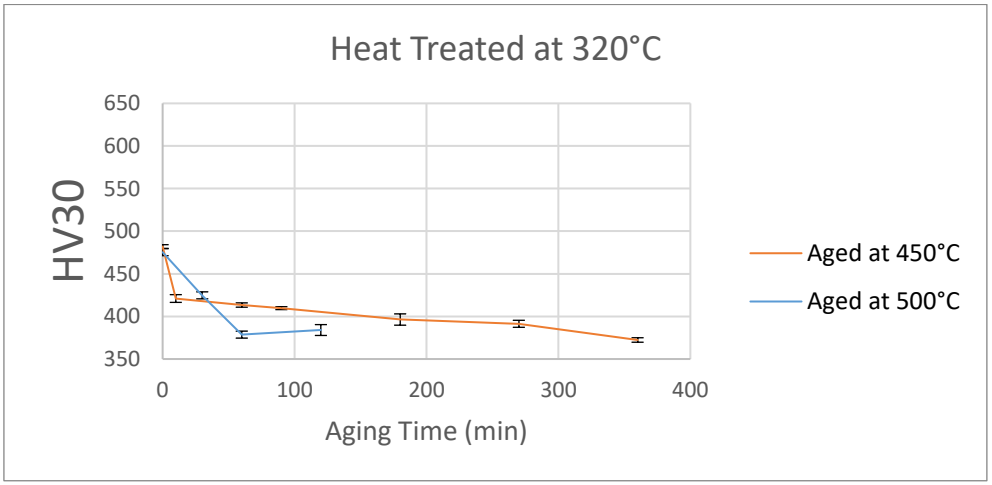

Figure 4.38. Superposition of Aging Time vs. Hardness Graph of Isothermally Heat-Treated Specimens at 320°C, then aged at 450°C & 500°C

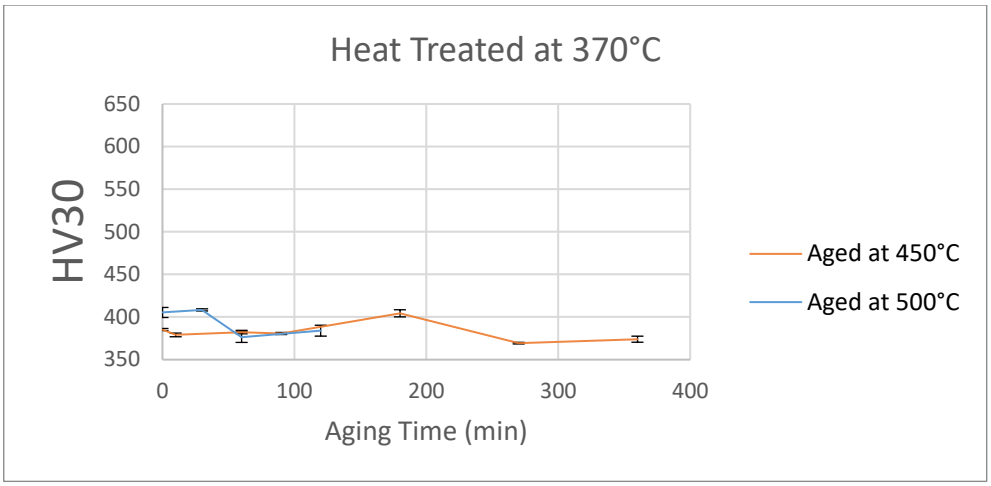

Figure 4.39. Superposition of Aging Time vs. Hardness Graph of Isothermally Heat-Treated Specimens at 370°C, then aged at 450°C & 500°C.

Depending on the work of Uzer [36], two different aging temperatures are selected, i.e., 450°C and 500°C. The specimens are aged between 10min-300min. Hardness values are tabulated in Table 4.6. Figures 4.28-4.35 show that all specimens' hardnesses decrease as aging time increases. This indicates that strength contribution from copper precipitates could not compensate for the softening effect of aging since aging also acts as tempering. In an isothermally treated specimen at 370°C, no change in hardness is observed after aging at either 450°C or 500°C. Hardness drop is more apparent for quenched and isothermally heat-treated samples at 170°C, 220°C, and 270°C. One explanation for this can be the difference between isothermal heat treatment and aging temperature: The bainite transformed at a higher temperature already has a coarse structure (in terms of bainite sub-unit width). Therefore, an aging treatment at 500°C or 450°C probably will have a minimal effect on microstructure. On the other hand, the finer microstructure of bainite which is transformed at a much lower temperature (i.e., for the specimens heat treated at 170°C, 220°C, and 270°C), will be affected from aging at 500°C to the larger extent. Another explanation for the larger hardness variation in isothermally treated specimens at 170°C, 220°C, and 270°C can be due to M/A contents. The M/A islands in all specimens are most probably martensitic

because retained austenite is not detected in any of the bainitic specimens. If the amount of martensite in specimens treated at 170°C, 220°C, and 270°C are higher, a drop in hardness in these specimens will be higher upon aging. This will be due to the tempering effect of aging. It is a well-known fact that the response of bainite to tempering is slow because the long transformation stages of bainite also act as auto-tempering [3, 38, 39]. Then a microstructure containing a higher amount of martensite will cause a larger hardness drop. Unfortunately, in a microstructure that consists of bainite + martensite, it is very difficult to differentiate bainite from martensite, especially if the isothermal transformation is carried out at a lower temperature. For this reason, strong evidence for the martensite/bainite ratios in specimens could not be found.

When the hardness values of aged specimens are compared, after an aging treatment at 450°C the hardness of all the specimens (i.e., 270°C, 320°C, 370°C) yield approximately 20HV higher values than that of the specimen aged at 500°C as indicated in Figure 4.37-4.39, this can be attributed to the low aging temperature of 450°C which softening takes at a slower rate.

Despite the decrease in hardness values obtained from the specimens heat treated at 170°C, 220°C, and 270°C, the specimens heat treated at 320°C, and 370°C seem unaffected from aging more than 1 hour, and even slight increase can be seen in Figure 4.36. Therefore, it can be deduced that copper precipitates may retard further softening and slightly increase strength in bainitic steels depending on bainitic transformation temperature.

CHAPTER 5

CONCLUSIONS

In this study, the effect of copper precipitation on 0.8%C steel was studied. To achieve this, the steel containing 0.8%C - 2%Cu-1%Ni was cast and then it is subjected to various heat treatments. The resulting samples were characterized by optical microscope, SEM, XRD and hardness measurements. The below conclusions are drawn from the results obtained in this thesis study.

1. Highest hardness values were obtained from as-quenched martensitic specimen (652HV) and from the isothermally treated specimen at 170°C (660HV).
2. When the isothermal transformation temperatures increase, hardness values of the specimens decrease. The hardness of specimen isothermally treated at 170°C yields 660HV. However, the hardness drops gradually to 405HV as the isothermal transformation temperature increases from 170°C to 370°C. This is attributed to the bainite sub-unit width which become thicker at high transformation temperatures.
3. Copper itself cannot suppress cementite formation in bainitic transformations. As a result, retained austenite could not be detected in isothermally treated bainitic specimens. In contrast, the quenched specimen yields around 5% retained austenite.
4. Bainitic specimens are aged at either 450°C or 500°C. Aging tough retard the softening of bainitic specimens, a secondary hardening peak could not be observed. Similarly martensitic specimens did not exhibit a secondary hardening peak upon ageing.

REFERENCES

[1] Ashby, M. F. (1989). Materials selection in conceptual design. *Materials science and technology*, *5*(6), 517-525

[2] Courtney, T. H. (2005). *Mechanical behavior of materials*. Waveland Press.

[3] Bhadeshia, H. K. D. H. (2019). *Bainite in steels: theory and practice*. CRC Press, pp.423-424.

[4] Miihkinen, V. T. T., & Edmonds, D. V. (1987). Fracture toughness of two experimental high-strength bainitic low-alloy steels containing silicon. *Materials Science and Technology*, *3*(6), 441-449.

[5] Sha, W., & Guo, Z. (2009). Maraging steels: modelling of microstructure. Properties and Applications, 63.

[6] Bhadeshia, H. K. D. H. (1998). New bainitic steels by design. *Modelling and simulation for materials design*, 227-232.

[7] Habraken, L., & Lecomte-Beckers, J. (1982). Hot shortness and scaling of copper-containing steels.

[8] Daehn, K. E., Cabrera Serrenho, A., & Allwood, J. M. (2017). How will copper contamination constrain future global steel recycling? *Environmental science & technology*, *51*(11), 6599-6606.

[9] Imai, N., Komatsubara, N., & Kunishige, K. (1997). Effect of Cu and Ni on hot workability of hot-rolled mild steel. *ISIJ international*, *37*(3), 224-231.

[10] Skoufari-Themistou, L., Crowther, D. N., & Mintz, B. (1999). Strength and impact behaviour of age hardenable copper containing steels. *Materials science and technology*, *15*(9), 1069-1079

[11] Laughlin, D. E., & Hono, K. (Eds.). (2014). *Physical metallurgy*. Newnes. (pp 1021-1068)

[12] Bhadeshia, H., & Honeycombe, R. (2017). *Steels: microstructure and properties*. Butterworth-Heinemann.

[13] Greninger, A. B., & Troiano, A. R. (1949). The mechanism of martensite formation. *JOM*, *1*(9), 590-598.

[14] Caballero, F. G., Santofimia, M. J., Capdevila, C., García-Mateo, C., & De Andrés, C. G. (2006). Design of advanced bainitic steels by optimisation of TTT diagrams and T0 curves. *ISIJ international*, *46*(10), 1479-1488.

[15] L. C. Chang and H. K. D. H. Bhadeshia: 'Microstructure of lower bainite formed at large undercoolings below bainite start temperature', Mater. Sci. Technol., 1996, 12, 233–236.

[16] E. Kozeschnik, H.K.D.H. Bhadeshia, "Influence of Silicon on Cementite Precipitation in Steels", Mater Sci Technol, vol. 24, pp. 343–347, 2008, https://doi.org/10.1179/174328408X275973.

[17] Soliman, M., & Palkowski, H. (2016). Development of the low temperature bainite. Archives of Civil and Mechanical Engineering, 16(3), 403–412.

[18] Garza-Martinez, L. G. (2003). Workability of 1045 forging steel with residual copper.

[19] Nakashima, K., Futamura, Y., Tsuchiyama, T., & Takaki, S. (2002). Interaction between dislocation and copper particles in Fe-Cu alloys. *ISIJ international*, *42*(12), 1541-1545.

[20] Kurdjumov, G. V., & Khachaturyan, A. G. (1975). Nature of axial ratio anomalies of the martensite lattice and mechanism of diffusionless γ→ α transformation. *Acta Metallurgica*, *23*(9), 1077-1088.

[21] Bain, E. C., & Paxton, H. W. (1966). Alloying elements in steel. *1966, 291 P. AMERICAN SOCIETY FOR METALS, METALS PARK, OHIO*.

[22] Krauss, G., & Marder, A. R. (1971). The morphology of martensite in iron alloys. *Metallurgical Transactions*, *2*(9), 2343-2357.

[23] Nicholson, R. (1972). *Strengthening methods in crystals*. halsted Press.

[24] Fielding, L. C. D. (2013). The bainite controversy. *Materials Science and Technology*, *29*(4), 383-399.

[25] H. J. Stone, M. J. Peet, H. K. D. H. Bhadeshia, P. J. Withers, S. S. Babu and E. D. Specht: 'Synchrotron X-ray studies of austenite and bainitic ferrite', Proc. R. Soc. A, 2008, 464, 1009–1027.

[26] F. B. Pickering: Transformations and Hardenability in Steels, p. 109, Climax Molybdenum Company, Ann Arbor, 1967.

[27] Zackay, V. F., Parker, E. R., Morris Jr, J. W., & Thomas, G. (1974). The application of materials science to the design of engineering alloys. A Review. *Materials Science and Engineering*, *16*(3), 201-221.

[28] Caballero, F. G., & Bhadeshia, H. K. D. H. (2004). Very strong bainite. *Current opinion in solid state and materials science*, *8*(3-4), 251-257.

[29] GARCIA-MATEO, C., & Caballero, F. G. (2005). Ultra-high strength bainitic steels. *ISIJ international*, *45*(11), 1736-1740.

[30] ASTM E3-11. (2017). Standard guide for preparation of metallographic specimens. *ASTM International*.

[31] Standard, A. S. T. M. (2017). ASTM E92-17 Standard test methods for Vickers hardness and Knoop hardness of metallic materials. *ASTM International.*

[32] Caballero, F. G., Garcia-Mateo, C., de Andr´es, C. G., 2005. Dilatometric study of reaustenitisation of high silicon bainitic steels: Decomposition of retained austenite. Materials Transactions 46, 581–586.

[33] Huang, H., Sherif, M., & Rivera-Díaz-Del-Castillo, P. (2013). Combinatorial optimization of carbide-free bainitic nanostructures. Acta Materialia, 61(5), 1639–1647.

[34] H.K.D.H. Bhadeshia, A.R. Chintha, S. Lenka, “Critical Assessment 34: Are χ (Hägg), η and ε carbides transition-phases relative to cementite in steels?”, Mater Sci Technol, vol. 35, no. 11, pp. 1301-1305, (2019).

[35] Fourlaris, G., Baker, A. J., & Papadimitriou, G. D. (1996). Effect of copper additions on the isothermal bainitic transformation in hypereutectoid copper and copper-nickel steels. *Acta materialia*, *44*(12), 4791-4805.

[36] Uzer, O. E. (2019). *The Aging characteristics of a medium carbon steel with and without copper* (Master's thesis, Middle East Technical University).

[37] Singh, S. B., & Bhadeshia, H. K. D. H. (1998). Estimation of bainite plate-thickness in low-alloy steels. *Materials Science and Engineering: A*, *245*(1), 72-79.

[38] Garcia-Mateo, C., Peet, M., Caballero, F. G., & Bhadeshia, H. K. D. H. (2004). Tempering of hard mixture of bainitic ferrite and austenite. *Materials Science and Technology*, *20*(7), 814-818.

[39] Kang, J., Zhang, F. C., Yang, X. W., Lv, B., & Wu, K. M. (2017). Effect of tempering on the microstructure and mechanical properties of a medium carbon bainitic steel. *Materials Science and Engineering: A*, *686*, 150-159.